Proceedings of the Fourth International Workshop

on

Laser ranging instrumentation

held at the
University of Texas in Austin, Texas, U.S.A.
October 12 – 16, 1981

Volume II

compiled and edited
by
Peter Wilson
President, Special Study Group 2.33, I.A.G.
Earth-satellite laser ranging

published by the
Geodetic Institute, University of Bonn, 1982

TABLE OF CONTENTS

THE LASER AND THE CALIBRATION OF THE CERGA LUNAR RANGING SYSTEM

by J.F. MANGIN, CERGA, France

The actual laser pulse width at half amplitude is 3 nanoseconds. In increasing the dye concentration, we can obtain 2.2 ns reliably.

The pulse energy is about 2.5 joules. The photon energy is :

$$h\nu = 6.6.10^{-34} . 3.10^{8} /0.7.10^{-6} = 2.8.10^{-19} J.$$

Then, each firing corresponds to 9.10^{18} photons. It is necessary to attenuate of 190 dB since the calibration requests "single photoelectron" event.

The target proximity forbids Flip-Flop use. Instead we have a beam splitter :

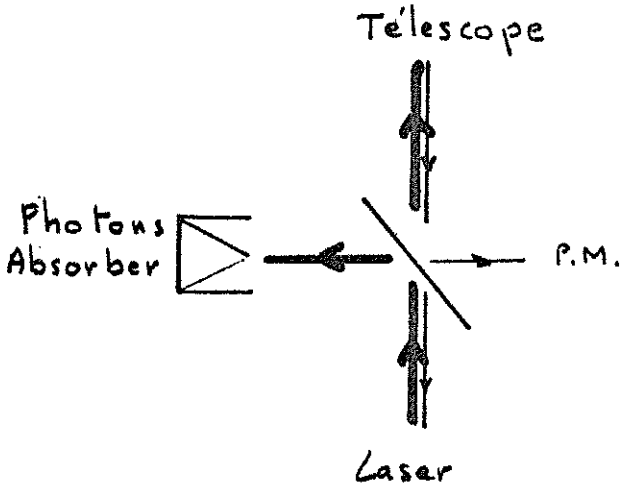

But this beam splitter permits many parasitic reflections on the P.M. (photon-absorber ; mirror II and various scattering) which could be very harmful.

To cure that and protect the laser, we decrease the laser output energy by switching-off the final amplifier. A part of the laser spot is retrieved from reflection on the final amplifier front face.

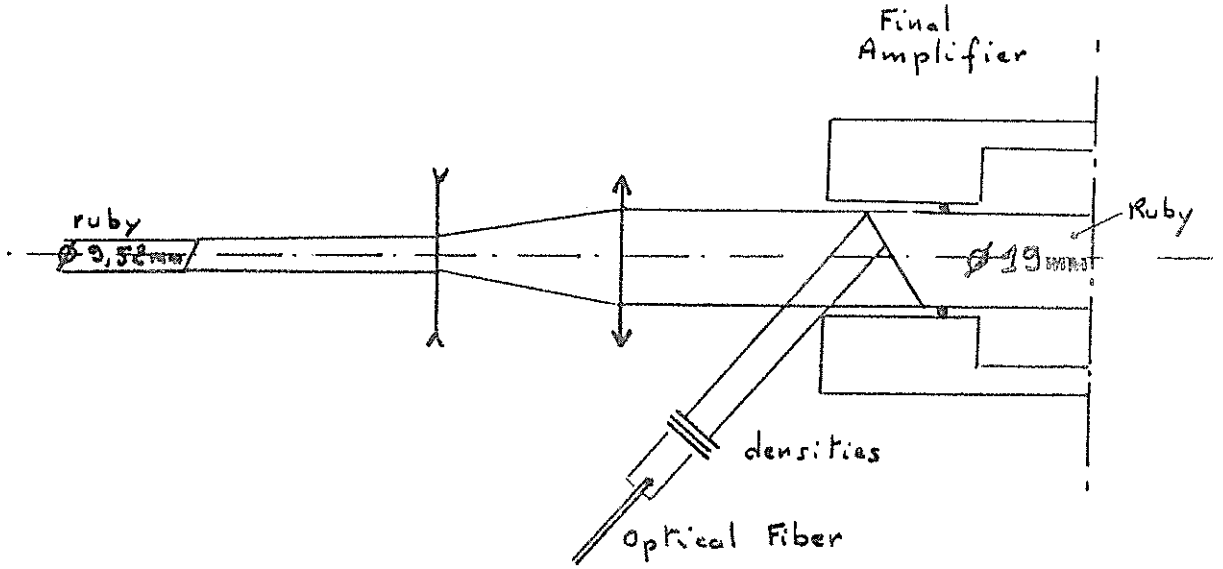

This pulse is directed via an optical fiber to the start pulse centroid detector. We have checked that energy collected by the optical fiber was independent of the final amplifier switching. Thus, the attenuation is 25 dB (5 dB : amplifier gain ; 20 dB : ruby absorption). Then, we can add 60 dB densities after the final amplifier. The target is a corner cube retro-reflector. Its aperture is a thousandth of the telescope's. So, we got 30 dB loss. Variable densities in front of the P.M. allow an attenuation from 0 dB to 80 dB. Thus it is possible to adjust the output level in order to receive statistically single photoelectron events.

The photomultiplier characteristics RCA 31034 A give 12 mV peak pulse for one photoelectron.

Reception diagram

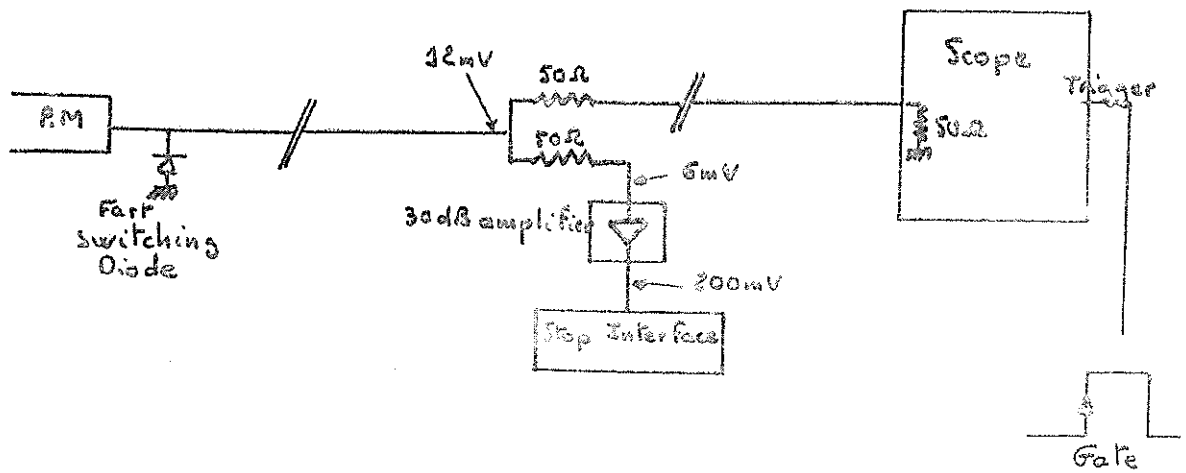

The separator allows a display on a fast storage oscilloscope of the returning event.

Start interface (fig. 1)

The start interface most provide the event-timer with a calibrated pulse synchronized with the center of the laser pulse. A start pulse centroid detector* is used. This allows to minimize the energy and width jitters of the pulse (inhomogeneity of the dicarbocyanine-methanol dye). We verified that, for a same laser pulse, two centroid detectors date this pulse with ± 120 ps r.m.s. delay. This integrator circuit is also used to display the energy of each firing by means of 7 L.E.D.

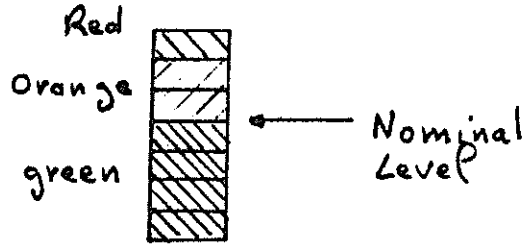

Stop interface (fig. II)

The stop interface realize several functions.

1/ Half amplitude detection, real time

Assuming that the P.M. output pulse corresponds to only one or several simultaneous photoelectrons, the half amplitude pulse width is about 4 ns. We did then an half amplitude detection dividing the amplitude by two and delaying the pulse by half its width. A comparator gives a calibrated pulse at the pulse crossing "A". Jitter from statistical gain gain variations of the P.M. are thus eliminated.

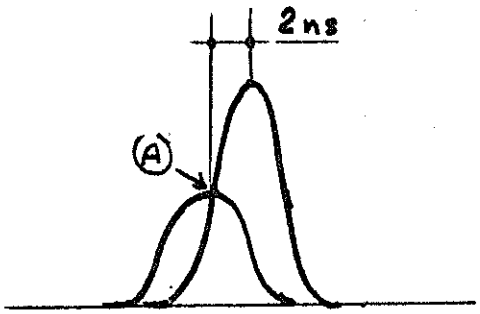

2/ Threshold setting, real time (J.M. TORRE, CERGA, France)

Post P.M. amplifier output pulse is compared with a variable level ranging from 150 mV (Moon ranging : one photoelectron about 200 mV) to 4 V (satellite ranging). A window allows to switch-on the signal only when it is above the threshold.

★ cf.: Third International workshop on laser ranging instrumentation "A start-Pulse Centroid detector", J-F Mangin and J. Gaignebet.

3/ Available output

An output from the processed pulses goes to a counter, allowing to know the noise under the experimental conditions.

4/ Gate

A signal from the "gate control" board allows transmission of the pulses to the event-timer if they are close to the predicted range. Gate width is adjusted manually from 20 ns to 50 µs by 20 ns steps.

It is possible to replace the threshold selector by a measuring system of the returning energy but the calibration target ranging did not show explicitly any correlation between the measurements and the returning pulse level if the detection works with few photoelectrons.

Calibration

- On June 17th, 1981, a calibration was realized on a target set up at Gréolière peak, 7 631.021 m distant from the mount axes crossing. The following histogram (fig. III) shows that measurements are distributed over 5 ns.

- On september 16th, 1981, two series of calibration were made, single and double round trip on the same target and one on the internal retroreflector (fig. IV, V, VI)

Calibration computing (Y. Boudon, CERGA, France).

On June 17th, 1981 : Cal. = 199.0 ns

On September 16th, 1981 :

- Single Round Trip : Cal. = 198,7 ns
- Double Round Trip : Cal. = 198,5 ns
- Silverberg method : Cal. = 198,7 ns
- Internal target : Cal. = 199,1 ns

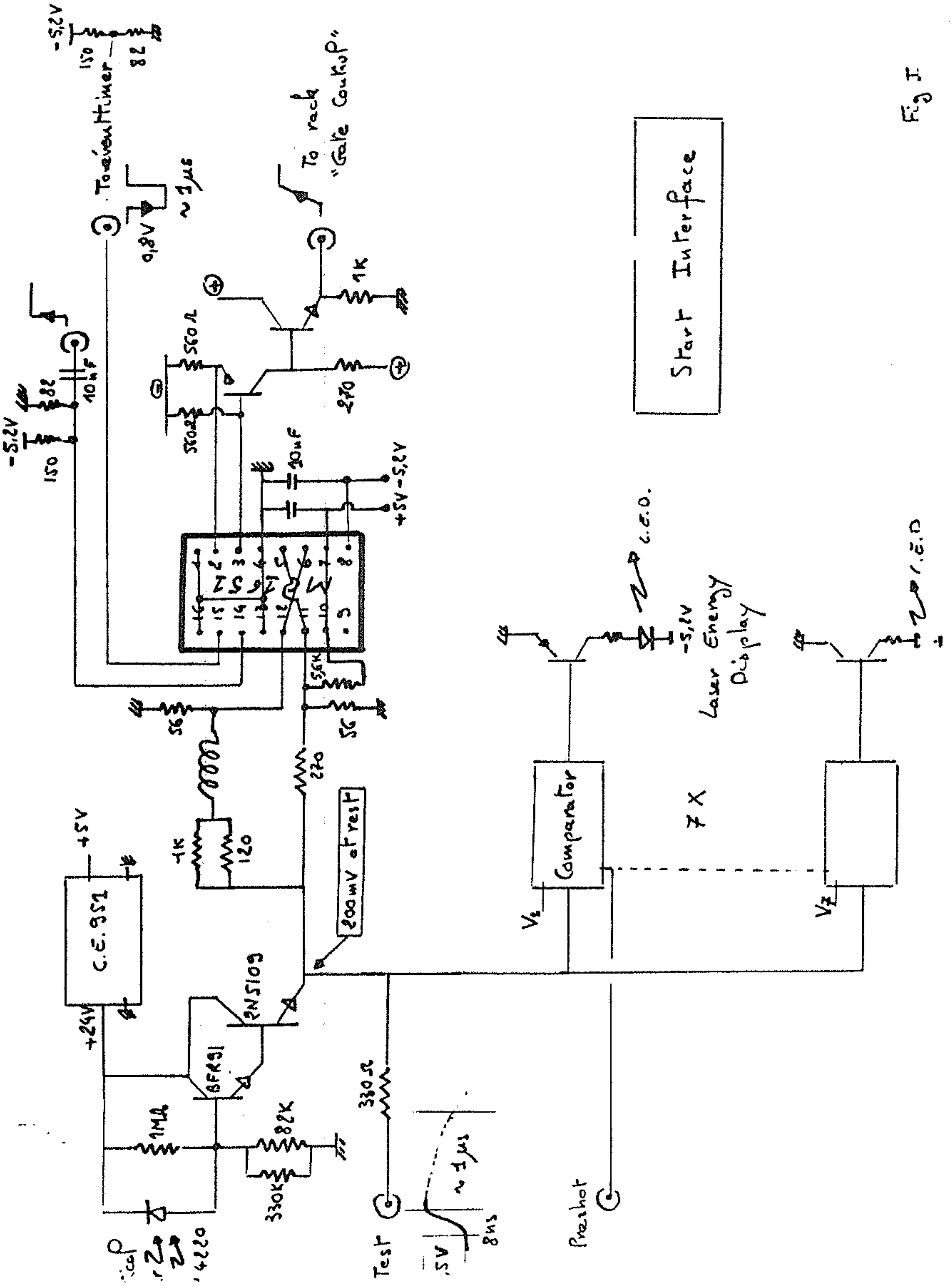
Start Interface
Laser Energy Display
Comparator
C.E. 952
2N5109
BFR91
200 mV at rest
Test
Preshot
7 X

Fig I

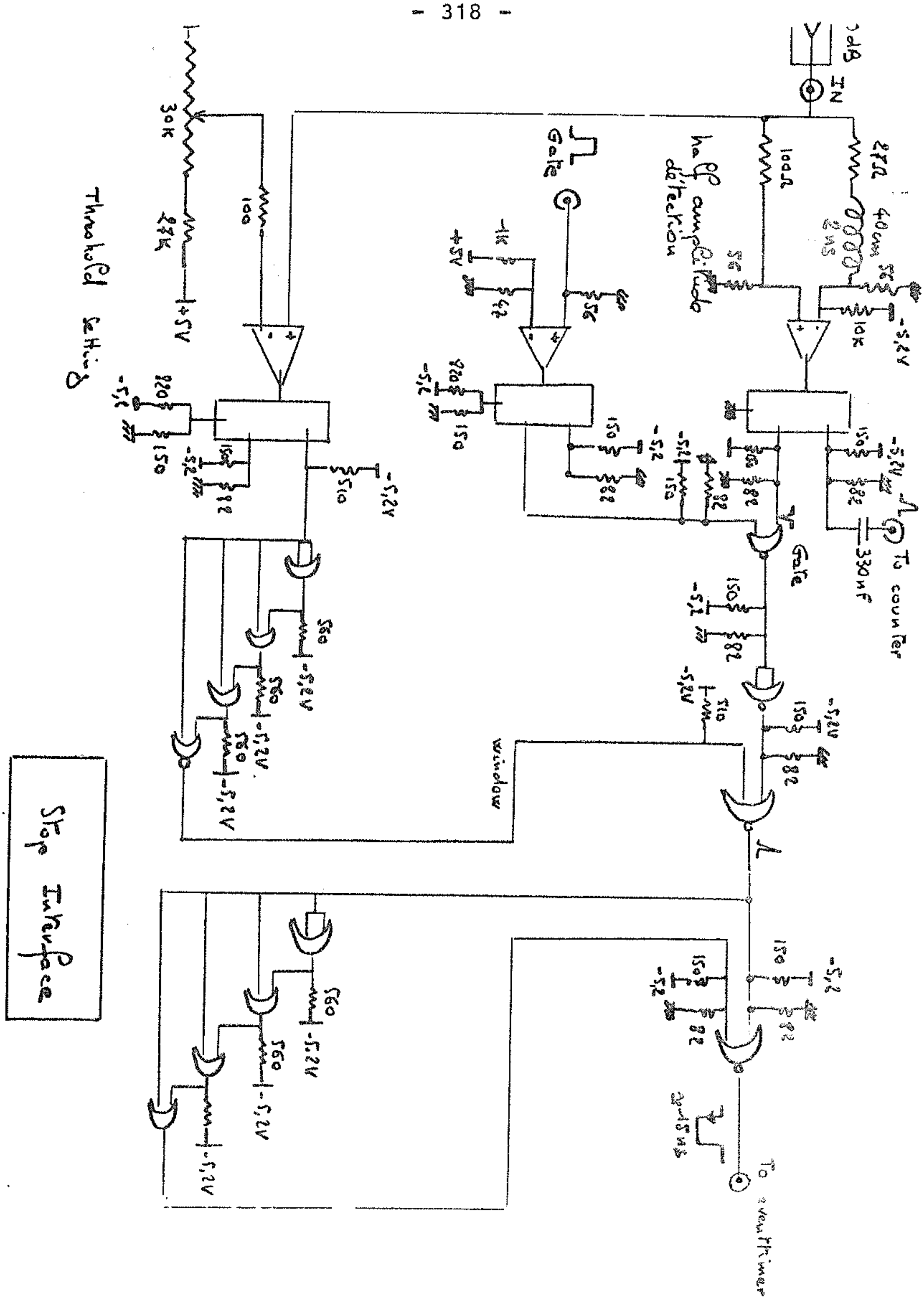
0dB
IN
half amplitude detection
Gate
To counter
Threshold setting
window
To eventtimer
Stop Interface

Fig II

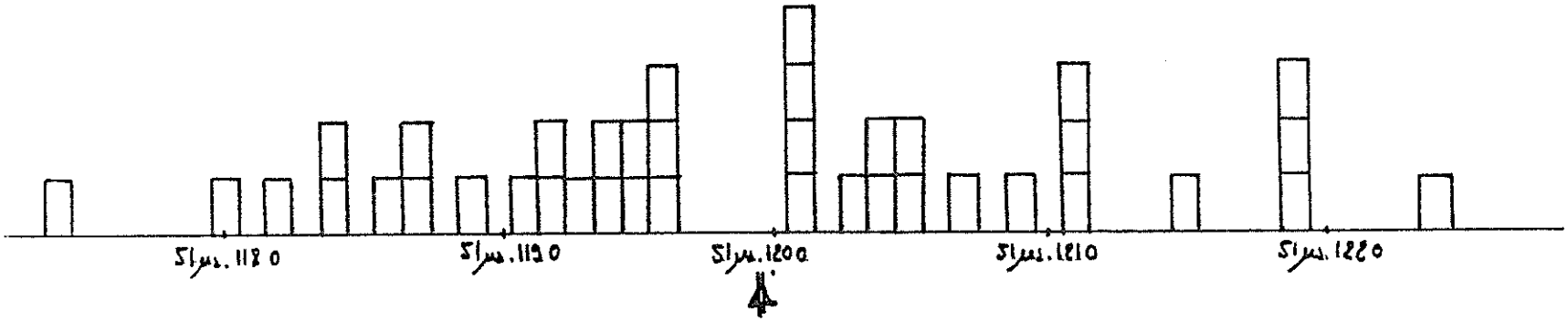

Calibration : Gréolière Target ; June 17th, 1981

T = 10,1°C D = 7631,021 m
P = 649,0 mm Hg d = 1.828 m

Asumed mean value 51µs. 119.9 | CoP = 199.0 ns

Fig. III

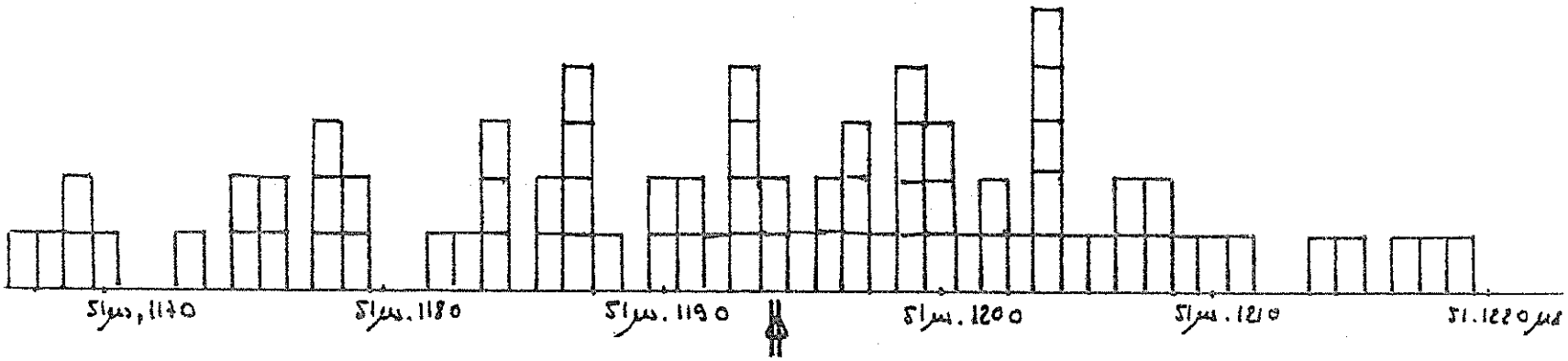

Calibration : Grésilleise Target ; September 14th, 1981

T = 16°5 C
P = 656 mm Hg

D = 7631,021 m
d = 1,806 m

Asumed mean value 51μs.1194 ⇒ **Cal = 198.7 ns**

Fig IX

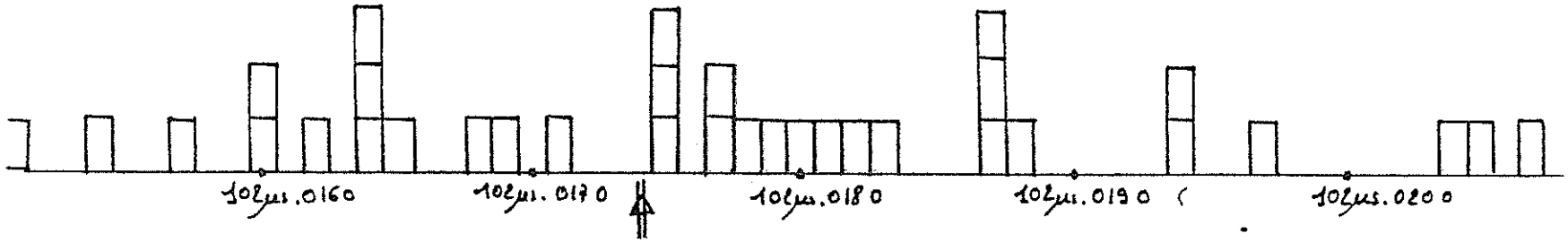

Calibration : Gréolière Target ; September 14th, 1981

T = 16,5 °C
P = 656 mm Hg

D = 7631,021 + (7631,021 - 3,387)
d = 1,806 + 1,806

Asumed mean value 102μs.017 4 ⇒ $\boxed{C_0P = 198.5}$

Fig IV

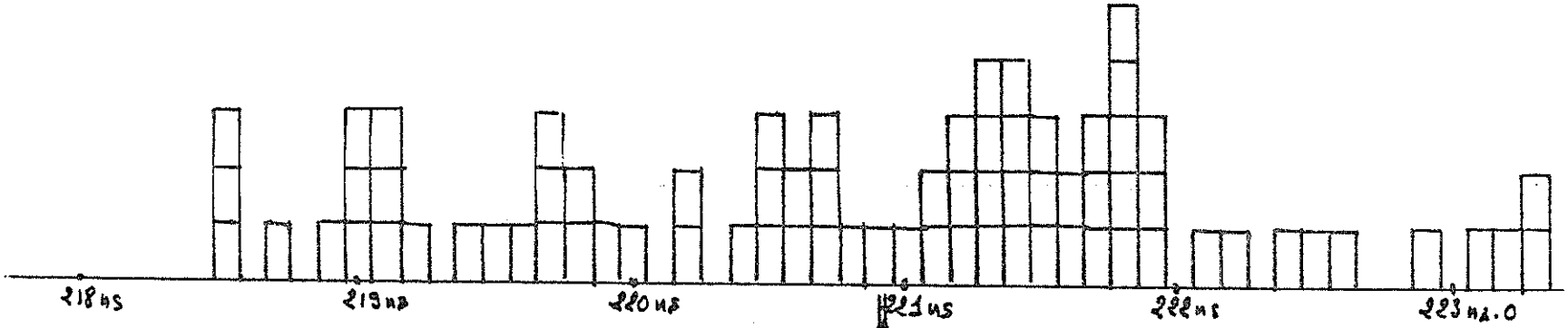

Calibration : Retroreflector September 16th, 1981

D= 3,263 m

Asumed mean value 220.9 ms ⇒ **CaP= 199.1 ms**

Fig VI

SAO CALIBRATION TECHNIQUES

M. PEARLMAN, N. LANHAM,
J. THORP AND J. WOHN

SMITHSONIAN ASTROPHYSICAL OBSERVATORY
CAMBRIDGE, MASSACHUSETTS 02138

Detailed and rigorous calibration procedures are the key to verifying system performance. In particular, as ranging accuracy requirements become more stringent the sources of data corruption become more illusive and more difficult to observe in ranging data. In fact, with the current state of geophysical models, it is unlikely that aliasing effects at the decimeter level would be recognized in long arc solutions. Calibration techniques may vary slightly depending upon system configuration. The techniques used by SAO are presented here as an example of the care that must be taken to ensure data quality and reliability. We also point out that these techniques were not invented by SAO but have evolved through experience by many participants in this field.

The SAO calibration procedures can be broken down into three categories: electronic calibration, specialized ground target calibration, and calibrations associated with satellite ranging procedures.

ELECTRONIC CALIBRATION

A full electronic calibration of the pulse processing system conducted several times per month and whenever a modification is made to the signal processing electronics provides the dependence of system delay on output pulse characteristics. It also provides a measure of electronic system jitter (post PMT). The calibration is performed by entering electronic pulses of widths 5, 6 and 7 nsec into both the output (start) channel and return (stop) channel circuitry. The input to the start channel is then varied +/-3 db from the normal operating level of the laser to encompass the effects of any variations in output signal strength that may be encountered during ranging. Regression analysis on this data gives the calibration parameter and a measure of the electronic system jitter (see Figure 1). Typical values for jitter range from .15-.20 nsec (2-3 cm). The calibration parameter and the jitter are monitored at both the stations and Headquarters to assess system performance.

Once per shift (usually at the beginning) the response of the 0.1 nsec resolution time interval counter is checked with a 100 msec period signal derived from the 1 MHz output of the station clock. Expected performance is +/-.1 nsec; 1 sigma scatter is typically 50-80 psec. Performance outside +/-.2 nsec indicates that the counter is not working properly.

SPECIALIZED TARGET CALIBRATIONS

Extended target calibrations on ground bill board targets are conducted at least once per month over the full operating range of the laser (1 - 1000 photoelectrons). This test is performed to monitor system calibrations as a function of signal strength to ensure that variations in system delay through the PMT and the pulse processing electronics are consistant with accuracy requirements. This measure also includes any long term drift effects in the system.

In practice, received optical signal strength is varied with neutral density filters in the photoreceiver to span the dynamic operating range. The calibration extends all the way down to the single photoelectron level where signal strength (pulse area) is determined from pulse counting statistics. This single photoelectron area is then used to calibrate signal strength over the full dynamic range. In the calculation, the data are divided up into subsets by

signal strength for convenience. Subsets have a minimum of 100 photoelectrons at the very lowest signal strengths and as many as several thousand at higher signal strengths.

An example of a calibration result is shown in Figure 2. In the present configuration, the calibration response is typically "flat" to better than +/-.4 nsec (6 cm). Error bars denote the standard deviation of the individual measurements.

The standard deviations are examined to assess the noise performance of the system (see Figure 3). In the intermediate regions we expect the sigma to follow a $1/\sqrt{n}$ dependence. At high signal strengths, sigma tends asymptomatically toward a fixed level characteristic of system jitter (electronic and PMT) which is typically .2 - .3 nsec. At very low signal strengths (~1 photoelectron) aside from effects of photon-quantization, the data also include corruption from degradation in pulse shape due to PMT response, and inadequate pulse sampling with the digitizer.

Ground target calibrations using a single retroreflector have been used to map the wavefront distortion of the laser. This distortion which arises from internal mode structure in the laser was particularly illusive because it could not be seen with the standard billboard target. Measurements of wavefront give us one of the fundamental limitations on the accuracy of a particular ranging system because in some cases error signatures may not be separable from geophysical effects.

In the calibrations taken by SAO, we probed the beam with a 3 by 3 or 4 by 4 matrix with a minimum of a 1000 photoelectrons (20 shots) at each point. See Pearlman, et al 1981. The results of a number of calibrations show a maximum variation of 9 cm across the beam with a r.m.s. variation of about 3 cm. The pattern of the wavefront distortion changes over a time period of several hours, but the magnitude values above are quite typical.

CALIBRATIONS ASSOCIATED WITH SATELLITE RANGING

To account for any possible changes or drift in system delay, calibrations are performed on the ground target before and after each pass. These precalibrations and postcalibrations, which consist of 20 points each at the 25 photoelectron level (for a total of 500 photoelectrons), are submitted with the pass data. System calibration is determined on a pass-by-pass basis as the mean value of the two calibration runs. The difference between precalibration and postcalibration values and the rms are used to estimate the short term system stability and the system noise. These numbers are monitored and compared with historical data. An example of calibration differences is shown in Figure 4. RMS calibration noise is typically .3 - .4 nsec as would be anticipated for a 6 nsec pulse.

In the process of ranging on satellites, we also record (digitize) several examples of the outgoing laser pulse. This is used for reference for centroid detection, and is also available for assessment of laser performance.

In all cases where the waveform is recorded (electronic calibration, target calibration, output pulse, satellite ranging, etc.), the digitizer baseline (or zeroset) is recorded for use in normalizing pulse shapes.

CONCLUSION

Calibration is an essential part of ranging. It should not be surprising that the laser in many cases must be fired as many times for calibration purposes as for ranging. On the otherhand, we must recognize that systematic errors can be extremely difficult to observe and that great care must be taken to design the hardware and the calibration procedures to isolate and measure these effects.

REFERENCES

Pearlman, M. R., N. W. Lanham, J. Wohn and J. Thorp, 1981. The Current Status and Upgrading of the SAO Laser Ranging Systems, to be presented at the Fourth International Workshop on Laser Ranging Instrumentation, Austin, Texas.

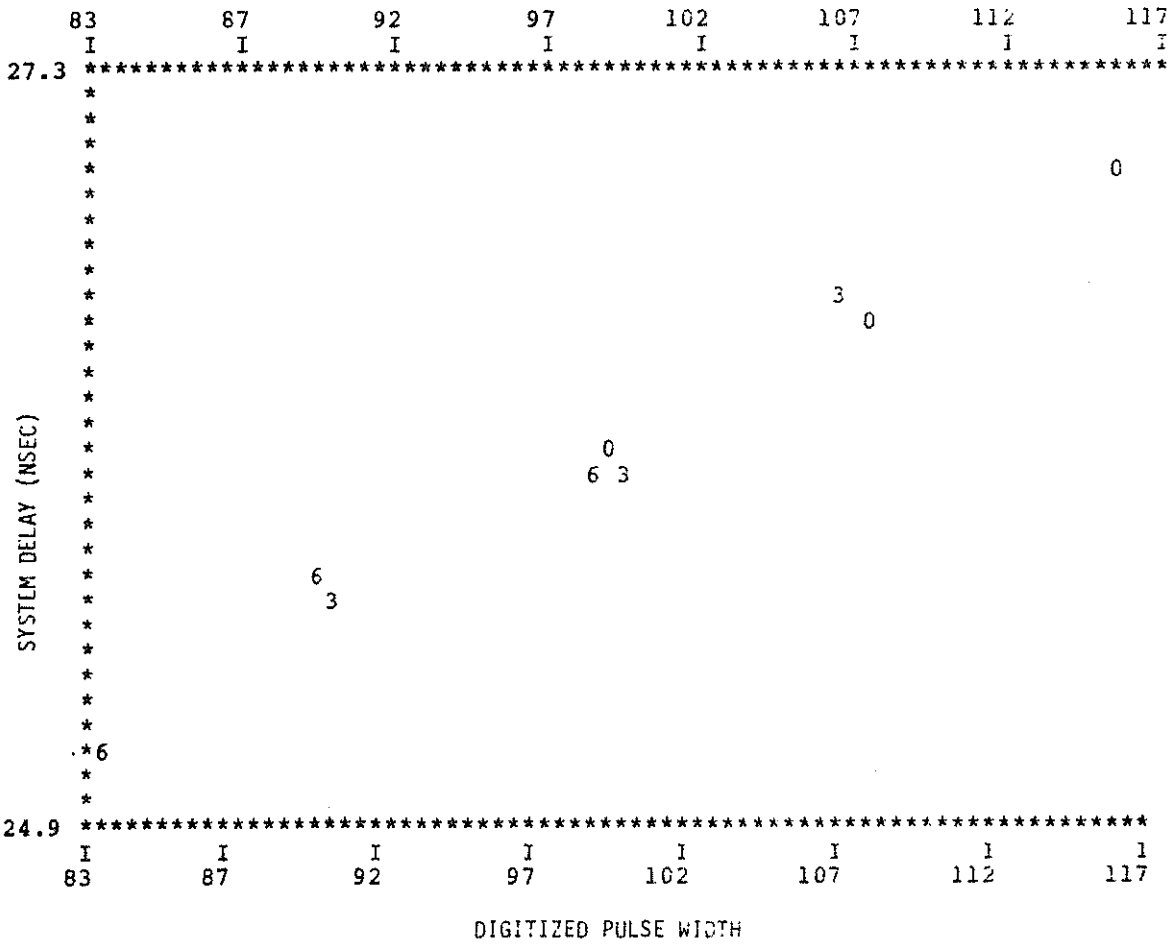

Figure 1.

Electronic system calibration showing change in start system delay with pulse width. Points on the graph represent averages of data sets taken at 5, 6 and 7 nsec with 0, 3 and 6db attenuation (denoted as 0, 3 and 6) in the signal line. The middle 3db point represents the nominal performance of the SAO laser with 6 nsec pulse width.

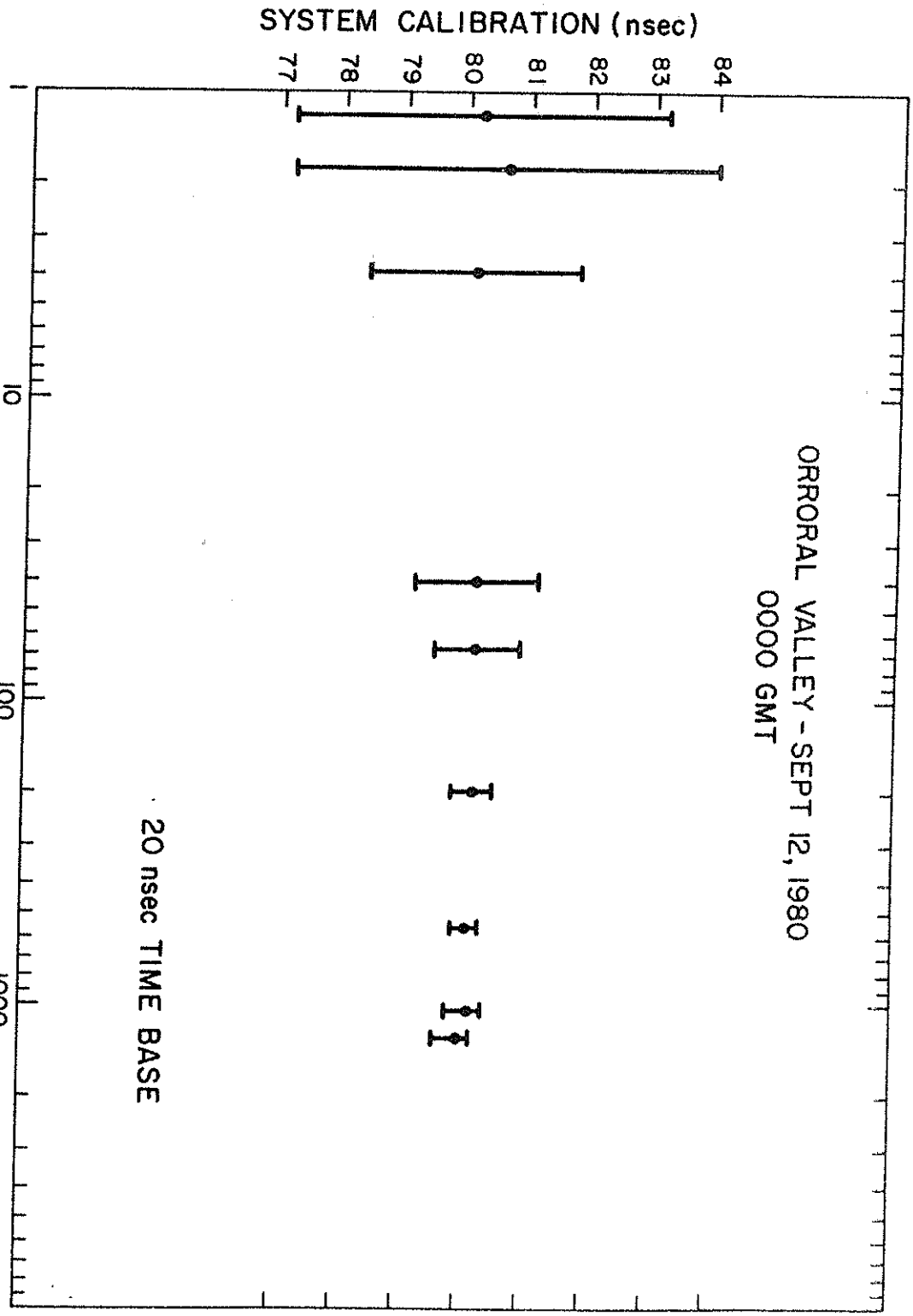

Figure 2.

Extended target calibration with single point uncertainties shown with brackets.

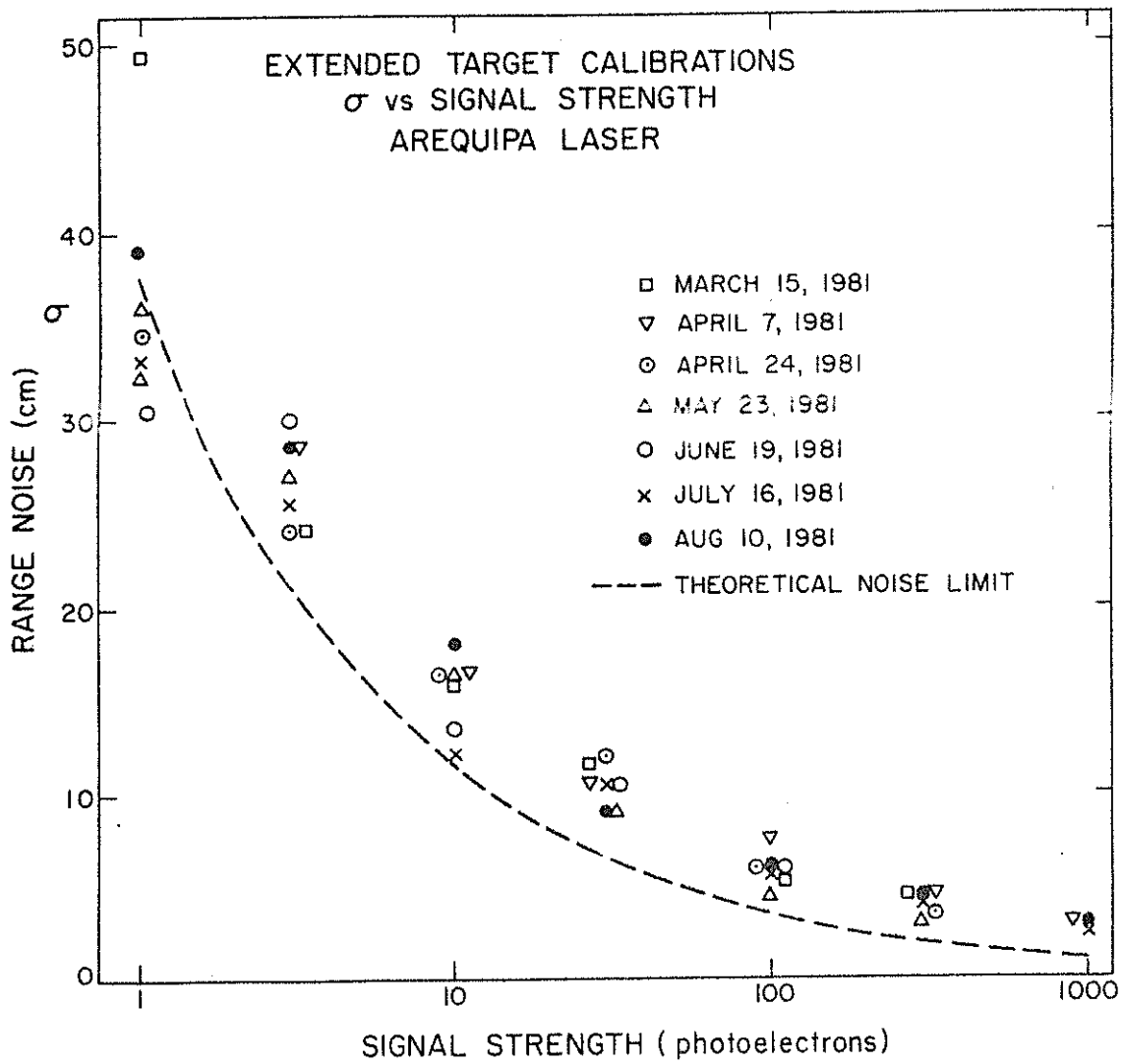

Figure 3.

Extended target calibrations, σ versus signal strength with theoretical limit shown.

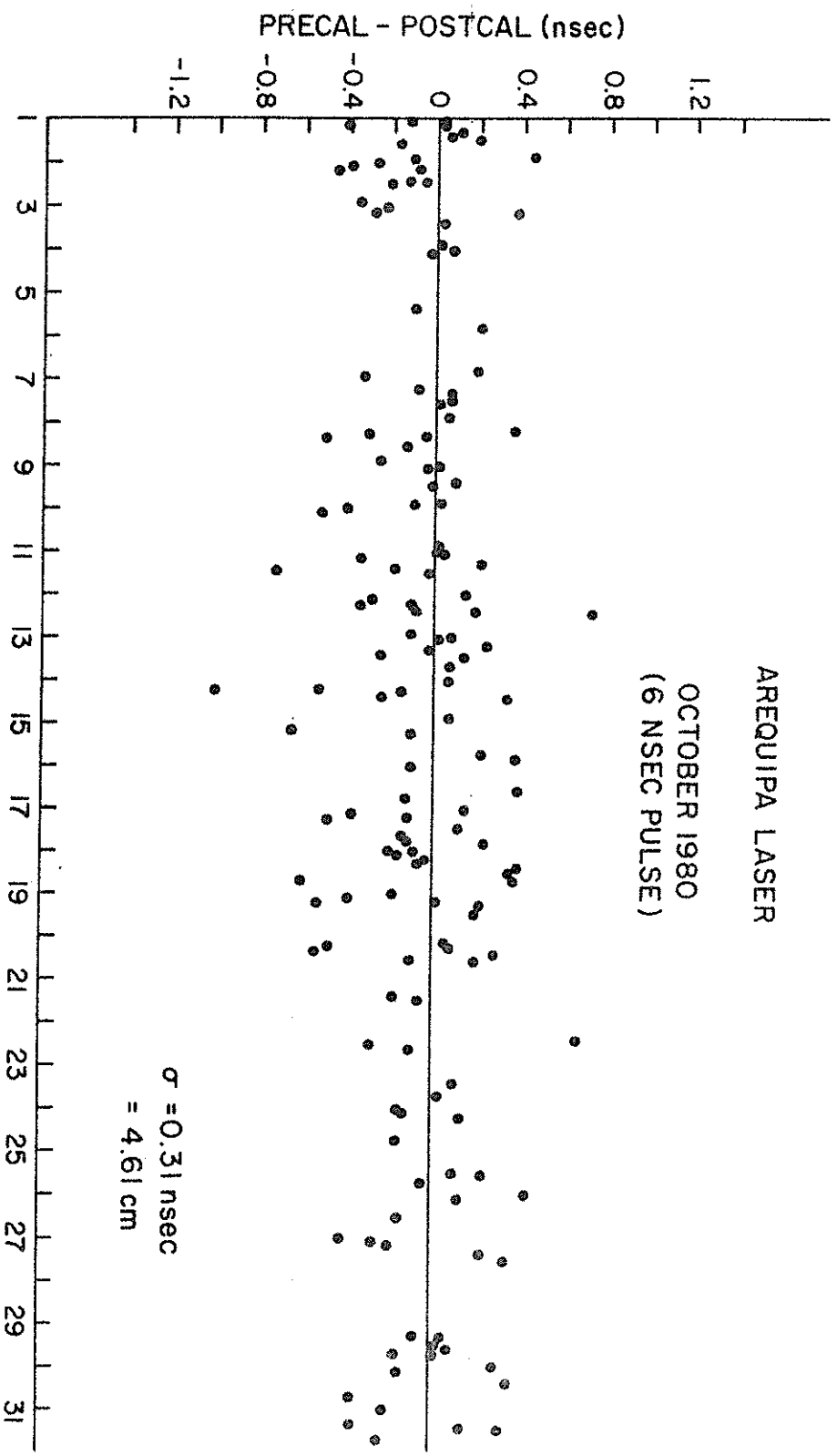

Figure 4.
Precalibration minus Postcalibration; 4 differences based on 20 shots each.

THE FEEDBACK CALIBRATION OF THE TLRS RANGING SYSTEM

BY

ERIC C. SILVERBERG
UNIVERSITY OF TEXAS McDONALD OBSERVATORY
AUSTIN, TEXAS 78712

The transportable laser ranging station (TLRS) which was constructed under a NASA Contract by The University of Texas, uses a multipulse mode-locked laser. The system relies on the use of real time feedback calibration to correct the time-of-flight data for the system delays. As such the system is truly self-calibrating, in the sense that it monitors the relevant system delays without operator interaction during each satellite pass.

The main features of this calibration scheme can be understood with the aid of Figures 1 and 2, the optical and electronic diagrams respectively. After the laser fires, a small amount of the output beam is diverted by an antireflection coated glass plate and immediately attenuated another factor of 10^6. It is then further attenuated to the single photoelectron level by a rotating attenuater which is located directly in front of the system spacial filter. Meanwhile, the signal from the system start diode travels through the discriminator circuitry and simultaneously starts the three system verniers which are contained in a commercial EG&G TD811 time digitizer unit. The start diode signal also latches the current epoch in a five megahertz, 28 bit circulating count register. The counter is phased by cable delays (D_3) to the TD811 to eliminate any 200 nsec ambiguities in the interpretation of the two readings. If a photoelectron pulse was created by the feedback light, it then travels through the discriminator units, through delay box D_1 to vernier 0. Vernier 1 of the TD811 stops

on the next 5 megahertz pulse which is delayed about 100 nanoseconds and also fed into vernier 2. (The program automatically selects the use of either vernier 1 or vernier 2 depending on which is closest to its mid-range.) All the verniers are, for convenience, adjusted to have the same slopes, but this is not absolutely necessary. The initial reading of vernier 0 is saved as the principal calibration constant.

When a return from the satellite travels through the system some tens of milliseconds later, the rotating mirror and rotating attenuater have moved to new positions so that the photons are routed through the spacial filter along the same path as the feedback. If a photoelectron is created, the latch again records the number of counts in the 5 megahertz counter, since the receiver "and" gate is open. The return photon also reactivates the start of the same TD811 used for the start sequence. In addition the return signal travels through the delay box to stop vernier 0. The true calibration constant i.e., the difference between the stop and start sides of the system is therefore $V_{01} - V_{02}$. By adjusting the length of the start cable, it is possible to hold $V_{01} - V_{02}$ close to 0 so that any error in the measurement of the vernier 0 calibration constant is not propagated into the range accuracies.

The time of flight is measured by the difference in the counter, as recorded by the two operations of the latch, plus the difference in verniers 1 and 2 which have been selected as mentioned earlier. Per usual, we correct the time of flight to that which would be measured if an infintessimally small telescope was observing from the first non-moving point on the receive path. This requires that we subtract twice the distance from the rotating mirror to the intersection of the axes (2a+2b+2d+2e+2f) and twice the additional size which the telescope implants from that point forward (2g). Note that the measurement of the path length from the beam splitter to the photomultiplier or from the beam splitter to the start diode is not important, since it affects both the calibration feedback path and the range path in exactly the same manner. The stability of the calibration vernier can, furthermore, be monitored independently by watching the numbers which are derived for V_{02}, since this merely represents a fixed cable delay.

So far all of these comments could be applied to any system which provides a feedback pulse which is at the same intensity as the satellite return. In the case of a single photoelectron system, however, the distribution in V_{01} will statistically build up the pulse shape of the laser system over a matter of hundreds of shots. We can use this information to not only determine the exact jitter which the total ranging system is undergoing at the time, but to further improve the accuracy of the results. Our calibration constant is removed by cross-correlating the array of $V_{01} - V_{02}$ readings with the array of returns from the satellite as plotted in residual space (o-c). This

allows the system to work with any laser pulse shape which can be monitored during a reasonable interval of time by the statistical sampling process. In the TLRS, for instance, a multiple pulse, dye mode-locked laser produces a return from the satellite such as shown in Figure 3a. When the data from this strong 3-minute burst was cross-correlated with the calibration data for that particular 3-minute span (3b), the cross-correlation function locates the calibration displacement with unerring accuracy. The point at which the calibration data and the returns from the satellite show the best match immediately realize the formation of a normal point which takes advantage of the full information available in the data. It also identifies with which laser pulse the returns should be identified and thus results in a calibration for each of the various return groups. When each return group was calibrated and folded together the resulting residuals form Figure 4. These data show an RMS deviation of approximately 8 centimeters.

The advantage of a real-time feedback calibration system is that it is capable of monitoring subtle pulse shape changes, discriminator settings and other factors during the actual ranging process thus preventing errors which might otherwise be possible. This is especially important in long duration LAGEOS runs where changing light levels, voltages and discriminator settings can make pre/post pass calibrations suspect. While it is bit more difficult to realize the real time calibration scheme than to calibrate off a target board, our experience in this area has been universally good and we recommend its use whenever possible.

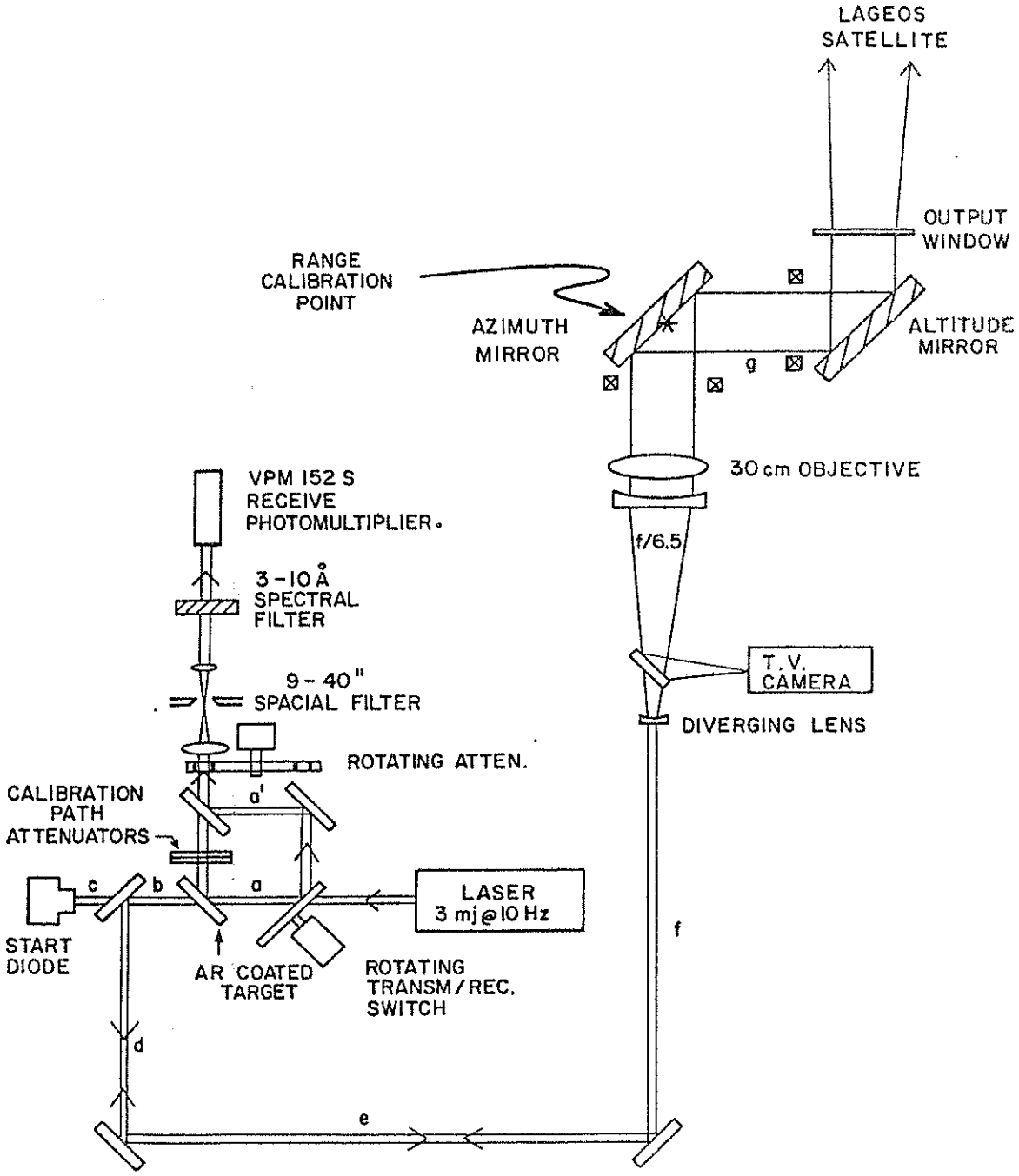

Figure 1: A schematic drawing of the major optical components in the TLRS.

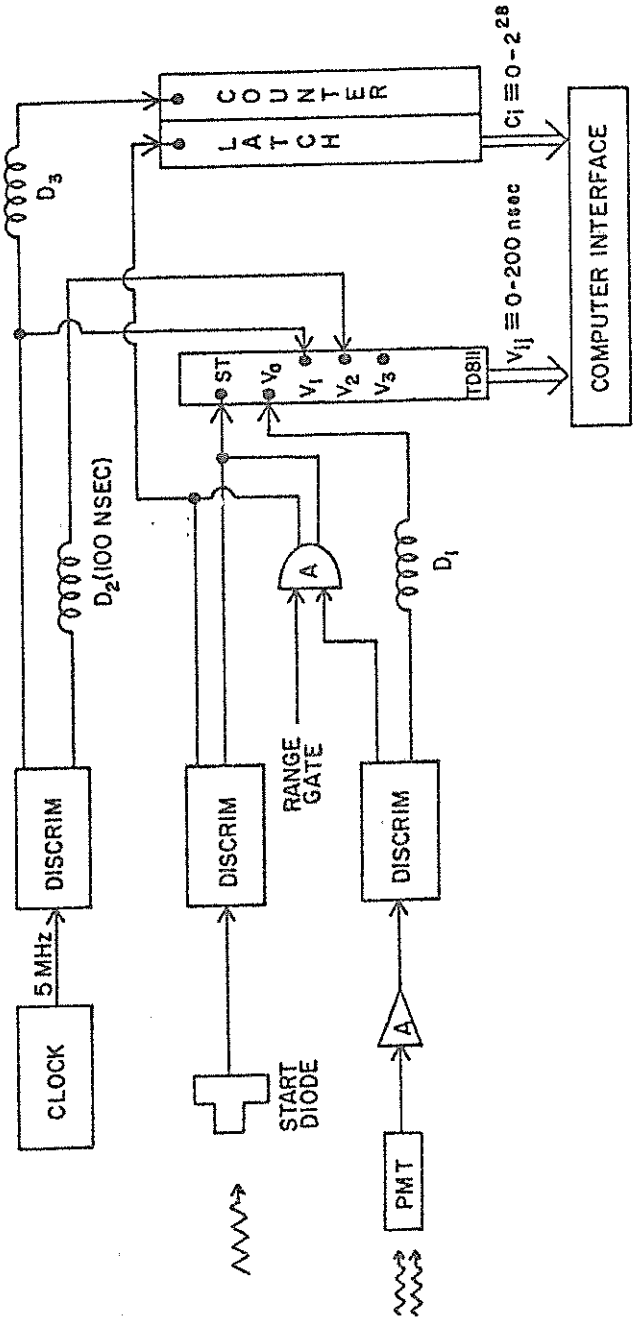

Figure 2: Shown is a schematic drawing of the critical components in the TLRS time-of-flight (TOF) system which are evolved in the real-time calibration scheme.

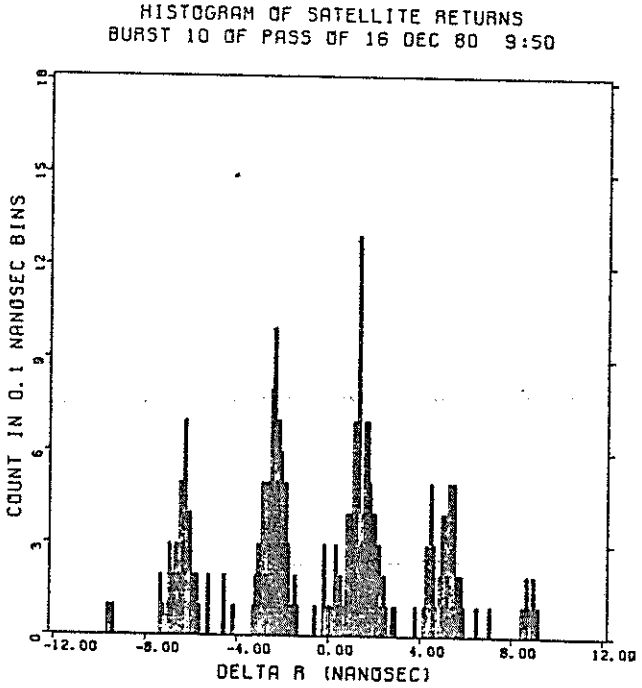

Figure 3(A): Shown is a histogram of the range residuals from a three minute burst on the LAGEOS satellite plotted relative to the average for the entire burst. Note the multipulse character of the laser and the fact that, in this case, the earlier pulses are slightly oversampled.

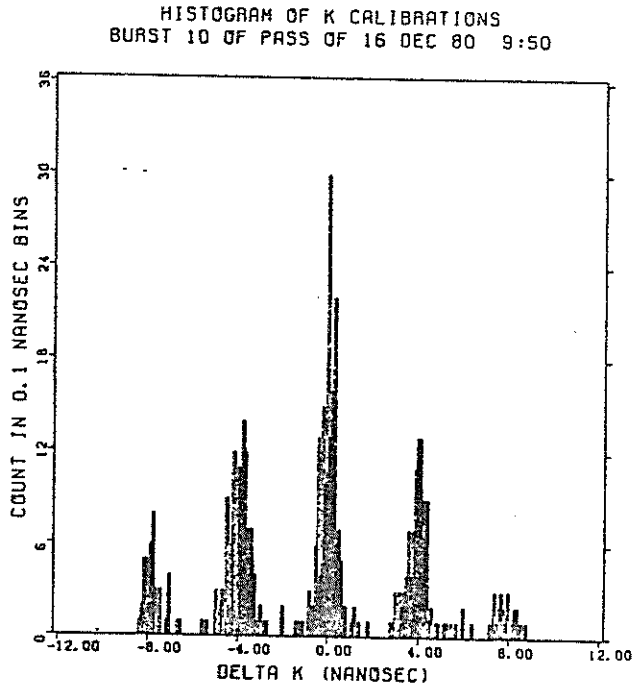

Figure 3(B): The feedback calibration data from the same time interval as in Figure 3(A) indicates not only the calibration bias, but also the true limitations of the system at that time.

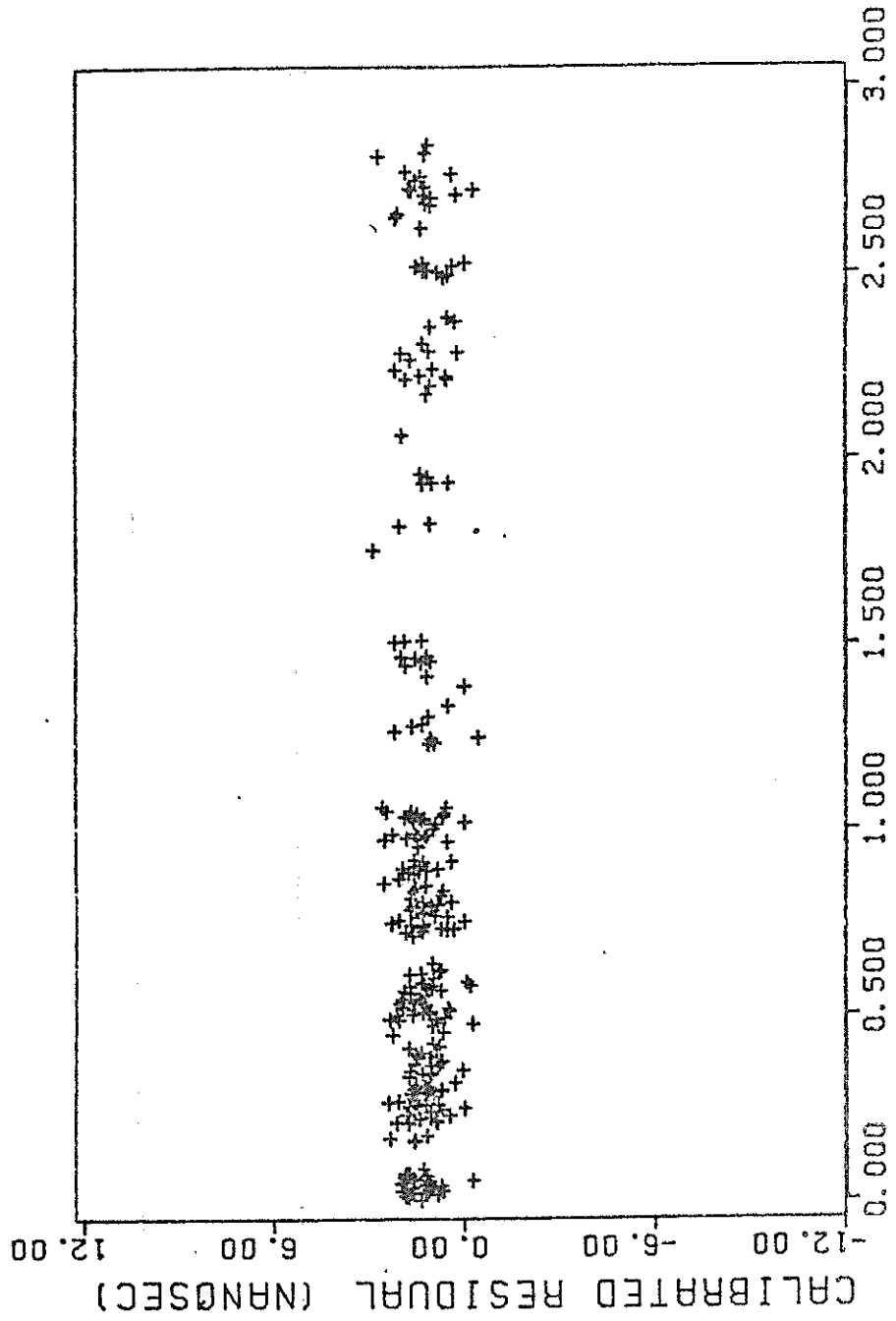

Figure 4: This drawing shows the calibrated residuals from the Figure 3 data. Good bursts show an RMS scatter of 7-8cm with as many as 550 returns.

GPS TIME TRANSFER RECEIVERS FOR THE NASA TRANSPORTABLE LASER RANGING NETWORK

O. Jay Oaks and James A. Buisson
Naval Research Laboratory
Washington, D.C. 20375

Schuyler C. Wardrip
NASA/Goddard Space Flight Center
Greenbelt, MD 20771

ABSTRACT

Present time synchronization techniques used within the Laser Network will be discussed. LORAN-C and portable clock data taken over the past year at various installations will be presented.

Future applications of the Global Positioning System (GPS) to achieve worldwide submicrosecond timing within the Laser Network will also be discussed.

The theme of the presentation will center on the performance of the NRL developed GPS receiver which was recently field tested at Kennedy Space Center, Florida. Portable clock measurements were made during the tests for comparison, with all measurements referenced to the Naval Observatory. Nine GPS timing receivers will be built for use in the Laser Network and other NASA facilities.

BACKGROUND

Present time synchronization techniques within the NASA laser network utilize LORAN-C and portable clocks. To use the highly accurate laser ranging data, it is necessary to time tag data from the laser stations very accurately. In applications where the data from two or more stations will be merged to determine baselines for geodetic work and polar motion determinations, it is necessary that the clocks at the several stations be synchronized to within ± 1 microsecond with respect to a master clock, such as that of the U.S. Naval Observatory (USNO). Best synchonization results using the LORAN-C system were obtained from the West Coast chain at the Goldstone, California laser tracking station (MOBLAS 3) and have an RMS of a half microsecond (Figures 1 and 2). Worst results have been a four microsecond RMS obtained in Australia (MOBLAS 5) using a wave hop from the Northwest Pacific chain (Figures 3 and 4). Portable clock measurements allow worldwide synchronizations of less than a microsecond but require frequent, therefore costly, travel to the remote stations.

Time transfers by satellite have been performed by NASA Goddard Spaceflight Center (GSFC) and the Naval Research Laboratory (NRL) initially using the NRL Navigation Technology Satellites (NTS).[1,2] Accuracies of several hundred nanoseconds were obtained.[3] As an outgrowth of the NTS effort, a Time Transfer Receiver (TTR) which operates with the NAVSTAR Global Positioning System (GPS) satellites is presently being developed jointly by GSFC and NRL. GSFC will

use the GPS TTR in the Laser Ranging Network. The network consists of eight mobile vans, a permanent installation at GSFC, and eventually four highly transportable laser systems. The laser systems will be deployed to various locations around the world (Figures 5 and 6) and will be used in support of the NASA GSFC Crustal Dynamics Program.

NAVSTAR GPS is a tri-service Department of Defense (DOD) program.[4] The first GPS satellite flown was NTS-II[5,6] which was designed and built by NRL personnel. GPS will provide the capability of very precise instanteous navigation and transfer of time from any point on-or-around the earth. At present six NAVSTAR satellites are on-orbit, providing instanteous navigation over selected areas for limited parts of each day. This constellation is part of the GPS Phase I configuration. Additional space vehicles (SV) are to be launched during the next year with the NAVSTAR 7 launch scheduled for December 1981.

The major objective of a satellite time transfer receiver is to determine precise time differences between a given satellite and a local ground clock referenced to the TTR (Figure 7). Precise time can then be obtained between the SV and a single remote ground station clock or between the SV and any number of remote stations. The remote sites could then be synchronized among themselves.

THE NAVSTAR GLOBAL POSITIONING SYSTEM (GPS)

GPS is comprised of three segments. The space segment consists of a constellation of satellites for global coverage.[7] Phase

III GPS will have a total of 24 satellites, eight in each of three orbital planes (Figure 8). The GPS orbits are near-circular at an altitude of approximately 10,000 nautical miles, inclined at 55 degrees to the equator. The period is adjusted such that a repeating ground trace is obtained for a given ground tracking station. Each satellite transmits its own identification and orbital information continuously. The GPS signal is spread spectrum in nature, formed by adding the data to a direct sequence code which is then biphase modulated onto a carrier.

The control segment consists of a master control station (MCS) and monitor stations (MS) placed at various locations around the world.(8) The current Phase I MCS is located at Vandenberg Air Force Base with the supporting monitor tracking stations at Alaska, Guam, Hawaii, and Vandenberg (Figure 9).

The monitor stations collect data from each satellite and transmit to the MCS. The data is processed to determine the orbital characteristics of each satellite and the trajectory information is then uploaded to each satellite, once every 24 hours as the spacecraft passes over the MCS.

The user segment consists of a variety of platforms containing GPS receivers which track the satellite signals and process the data to determine position.(9,10) Coverage of the Phase III constellation is such that at least four satellites will always be in view from any point on the earth's surface.

TIME TRANSFER METHOD

To perform a satellite time transfer with GPS, pseudo-range measurements are made that consist of the propagation delay in the signal plus the difference between the satellite clock and the ground station receiver reference clock. Data from the satellite is processed to obtain satellite position and satellite clock information (offset from GPS time). The propagation delay is subtracted from the pseudo-range by knowing the exact locations of the satellite and the station. This result is then corrected by the GPS time offset to determine the final result of ground station time relative to GPS time. The Phase I GPS time is maintained at the Vandenberg MCS using a cesium oscillator. The Phase III GPS time is planned to be referenced from the MCS to the U. S. Naval Observatory (USNO) Master Clock. The final results obtained from a single-frequency receiver, such as the one described in this paper, will contain a small error due to the ionospheric delay which may be modeled and corrected.

GPS TIME TRANSFER RECEIVER (TTR)

The GPS TTR is a microcomputer based system which was designed to replace existing receivers that formerly used the NTS satellites for time transfer. The design used hardware and software from these receivers whenever possible. The following is a summary of the design requirements:

A. GPS Signal Detection Characteristics

1) Operates at the single L1 frequency of 1575 MHz

2) Has sufficient bandwidth to track satellites throughout their doppler range from horizon to horizon

3) Uses only the course/acquisition (C/A) code of 1.023 MHz

4) Tracks the C/A code to within 3% of a chip (30 nanoseconds)

5) Tracks any GPS satellite by changing to the appropriate code

6) Detects and decodes the navigation data as required to determine a time transfer

B. Operational Characteristics

1) Requires a stationary platform during operation

2) Determines the time difference between the 1 pps input station reference and GPS system time

3) Measures the time difference once every six seconds

4) Has an RMS of less than 50 nanoseconds on the time difference measurements

5) Controls the operation of the receiver by inputs from a keyboard

6) Outputs data to the CRT display and records on a flexible disc

C. Input Requirements

1) Antenna position in WGS-72 coordinates

2) 1 pps from the station time standard

3) 5MHz from the station time standard

With these design requirements, the receiver block diagram in Figure 10 was implemented. The following is a description of the major components shown in the diagram.

RF SUBSYSTEM

The RF subsystem provides carrier and code tracking capabilities for the GPS signal. It demodulates the data message into the non-return to zero (NRZ) format and provides the voltage controlled crystal oscillator (VCXO) frequency for coherent code generation. An external control voltage input to the VCXO is used for acquisition tuning.

C/A CODE GENERATOR

The C/A code generator accepts the code sequence of any GPS satellite from the microprocessor. It then derives the 1.023 MHz C/A code from the VCXO frequency and outputs it to the RF subsystem for code tracking. A satellite time epoch is derived from the C/A code period and output for the time interval psuedo-range measurement.

TIME INTERVAL MEASUREMENT

A time interval counter is controlled by the microprocessor to measure the time difference between the satellite epoch and the station reference. This measurement occurs once every six seconds as commanded by the microprocessor. The time difference, which is psuedo-range, is output to the microprocessor for determining the time transfer. The time interval counter is also used to determine the VCXO frequency for tuning control.

I/O TERMINAL

The receiver contains a CRT display with a keyboard and a dual flexible disc drive recorder. Operator control of the receiver is through keyboard inputs. The time transfer results are displayed on the CRT and recorded on the flexible disc.

MICROPROCESSOR

The microprocessor controls hardware functions in the receiver, decodes the navigation message, and calculates the time transfer. Receiver tuning is provided during acquisition by taking frequency measurements of the VCXO, comparing these measurments to predicted values and outputing corrections to the control voltage through a digital-to-analog converter.

The appropriate satellite C/A code is loaded into the code generator after being calculated using a linear feedback shift register algorithm implemented in the microprocessor. The code phase is also controlled by the microprocessor until a correlation or "code lock" is established in the RF subsystem. After signal acquisition, the microprocessor decodes the navigation data and commands pseudo-range measurements to be performed using the time interval counter to calculate the final time transfer result. This result is output to the CRT display and recorded on a flexible disc once every six seconds.

TIME TRANSFER FIELD TEST

The prototype GPS TTR was installed and tested at NASA's Merrit Island tracking site (MILA) at Kennedy Spaceflight Center, Fla.

Figure 11 shows the horizon of the MILA facility and the portion of the orbit of NAVSTAR 5 in view at the MILA site. Figure 12 shows the orbits of all five NAVSTAR satellites along with approximate rise and set times for the period during which the tests were performed. Most of the data was taken during a segment of time when all the satellites passed through a high elevation angle (60° to 90°) with approximately the same azimuth. Figure 13 shows the segments of each orbit where the data collection was concentrated. Figures 14 through 18 present the clock difference between the MILA station ground clock and the GPS spacecraft clocks as determined from individual satellite passes observed during the test. On each graph a calculated time transfer is presented for an epoch close to the mid-time of the observed period. The RMS of a least squared data fit is also presented. The RMS of any one pass varies from 11 to 13 nanoseconds for a given satellite.

Figure 19 is an extended track (two hour) of a NAVSTAR 6 pass. NAVSTAR 1 has a quartz crystal oscillator, NAVSTAR 3 and 4 have rubidium oscillators, while NAVSTAR 5 and 6 have cesium oscillators.

Figure 20 shows the time transfer results taken through each satellite and referenced to USNO master clock over a seven day period. Figure 21 shows the same results as an equal weighted average of all satellites. Results from individual satellites appear to vary as much as several hundred nanoseconds. The most well-behaved data on a day-to-day basis is that obtained from NAVSTAR 5. Figure 22 shows a comparison

of the five satellite average results with measurements made through LORAN-C and with portable clock measurements referenced to the U.S. Naval Observatory Master Clock.

Even though, during Phase I of the GPS, no attempt is being made by the MCS to precisely synchronize the five NAVSTAR space vehicles (SV), the results of the GPS data taken on all SVs during this experiment compares to the portable clock data to within 200 nanoseconds. It is planned during Phase III to maintain SV synchronization to within 100 nanoseconds.

Improvements were made to the receiver as a result of this field test, and data has subsequently been taken at NRL. Figure 23 is a typical plot of data taken from NAVSTAR 4 over a period of 22 days. A fit to this data produces a 25 nanoseconds RMS over the observed time period.

SIRIO/LASSO TIME TRANSFER EXPERIMENT

Future activities include joint participation by GSFC, USNO, and NRL in the European Space Agency (ESA) SIRIO/LASSO time transfer experiment during 1982. The missions of SIRIO-2 are twofold; meteorological data dissemination and synchronization of intercontinental atomic clocks.

The aim of the LASSO experiment is to provide a repeatable near-real-time method for long-distance (intercontinental) clock synchronization with nanosecond accuracy at a reasonable cost. The pioneering aspects of this first experiment will provide the opportunity to compare

the international network of atomic clocks with the internationally adopted atomic time scale (TAI) and with each other. It will also have an impact on such practical applications as the tracking of deep space missions, the calibration of other time transfer techniques such as Very Long Baseline Interferometry (VLBI), Tracking Data Relay Satellite System (TDRSS), the Global Positioning System (GPS), and future generations of space navigation and telecommunciation systems.

SIRIO-2 will be launched during March of 1982 from Koarou, French Guiana in South America into a synchronous orbit at 25 degrees west longitude, just off the West Coast of Central Africa near Liberia (Figure 24). The satellite has a 2-year lifetime design and will remain in this position for about 9 months to permit time measurments between the United States (Goddard Space Flight Center referenced to the Naval Observatory) and major observatories and time keeping facilities in Europe--principally with the Bureau International de l'Heure (BIH) in Paris, France. SIRIO-2 will then be moved over Central Africa at 20 degrees east longitude and will remain there for meteorological data dissemination until the completion of its 2-year mission.

SPACECRAFT CHARACTERISTICS

The LASSO experiment is based on the use of laser ground stations firing monochromatic light pulses at predicted times directed toward the geosynchronous SIRIO spacecraft.

SIRIO-2 is a spin-stabilized geostationary satellite spun around an axis vertical to its orbital plane (Figure 25). The spacecraft

consists of a drum-shaped central body covered with solar cells. On top is mounted a mechanically despun S-Band (1689.6 MHz) antenna for support of the meteorological, timing missions, and housekeeping data. Omnidirectional antennas (VHF 136.14 MHz) serve for command, ranging and backup telemetry.

The LASSO payload is composed of retroreflectors, photodetectors (for sensing ruby and neodyme laser pulses), and a stable clock for time tagging arrival times of laser pulses.

LASSO EXPERIMENT GOALS

The goals of the LASSO experiment are as follows:

1. Verify that lasers can be used to perform a two-way time transfer from a geostationary satellite to within nanoseconds or sub-nanoseconds.
2. Determine the limations and problems of such a laser time transfer technique.
3. Verify the accuracy of other techniques, such as the Global Positioning System (GPS) time transfer technique, using receivers being developed for use in the Mobile Laser Network.

FUTURE PLANS

Increased receiver performance and capabilities development is continuing based on results and operational feedback from field tests and on-going experiments. Extensive evaluation of the receiver

is planned through several additional field tests. A joint experiment is scheduled with the Jet Propulsion Laboratory (JPL), to evaluate ionospheric delay error. Co-location tests are planned to compare nanosecond accuracy VLBI data with GPS TTR data. The co-location tests will involve VLBI stations at NRL Maryland Point, Haystack/ Westford Observatory, NASA Deep Space Network (DSN), Goldstone, CA., and NASA DSN, Madrid, Spain. Analysis will also be performed from the data obtained during the SERIO/LASSO experiment.

The first operational field test of the GPS TTR is scheduled in the second quarter of fiscal year (FY) 1982 with the deployment of the NASA GSFC Transportable Laser Ranging System (TLRS) prototype to Easter Island. Four additional receivers are scheduled to be deployed with mobile laser systems later in FY 1982.

REFERENCES

1. L. Raymond, O. J. Oaks, J. Osborne, G. Whitworth, J. Buisson, P. Landis, C. Wardrip, and J. Perry, "Navigation Technology Satellite (NTS) Low Cost Timing Receiver," Goddard Space Flight Center Report X-814-77-205, Aug. 1977.

2. J. A. Buisson, T. B. McCaskill and O. J. Oaks, "Initial Design for Navigation Technology Satellite Time Transfer Receiver (NTS/TTR)," NRL Report 8312, 16 May 1979.

3. J. Buisson, T. McCaskill, J. Oaks, D. Lynch, C. Wardrip, and G. Whitworth, "Submicrosecond Comparisons of Time Standards via the Navigation Technology Satellites (NTS)," Proc. PTTI, Nov. 1978, pp 601-627.

4. B. W. Parkinson, "NAVSTAR Global Positioning System (GPS)," National Telecommunications Conference, Conference Record, Vol. iii, 1976, pp 41.1-1 to 41.1-5.

5. J. A. Buisson, R. L. Easton, and T. B. McCaskill, "Initial Results of the NAVSTAR GPS NTS-2 Satellite," NRL Report 8232, May 25, 1978.

6. R. L. Easton, J. A. Buisson, T. B. McCaskill, O. J. Oaks, S. Stebbins, and M. Jeffries, "The Contribution of Navigation Technology Satellites to the Global Positioning System," NRL Report 8360, Dec. 28, 1979.

7. J. A. Buisson and T. B. McCaskill, "TIMATION Navigation Satellite System Constellation Study," NRL Report 7389, June 27, 1972.

8. S. S. Russel and J. H. Schaibly, "Control Segment and User Performance," J. Inst. Navigation 25(2), Summer 1978, pp. 166-172.

9. J. J. Spilker, "GPS Signal Structure and Performance Characteristics," J. Inst. Navigation, 25(2), Summer 1978, pp. 121-146.

10. A. Dierendock, S. Russell, E. Kipitzke, and M. Birnbaum, "The GPS Navigation Message", J. Inst. Navigation, 25(2), Summer 1978, pp. 147-165.

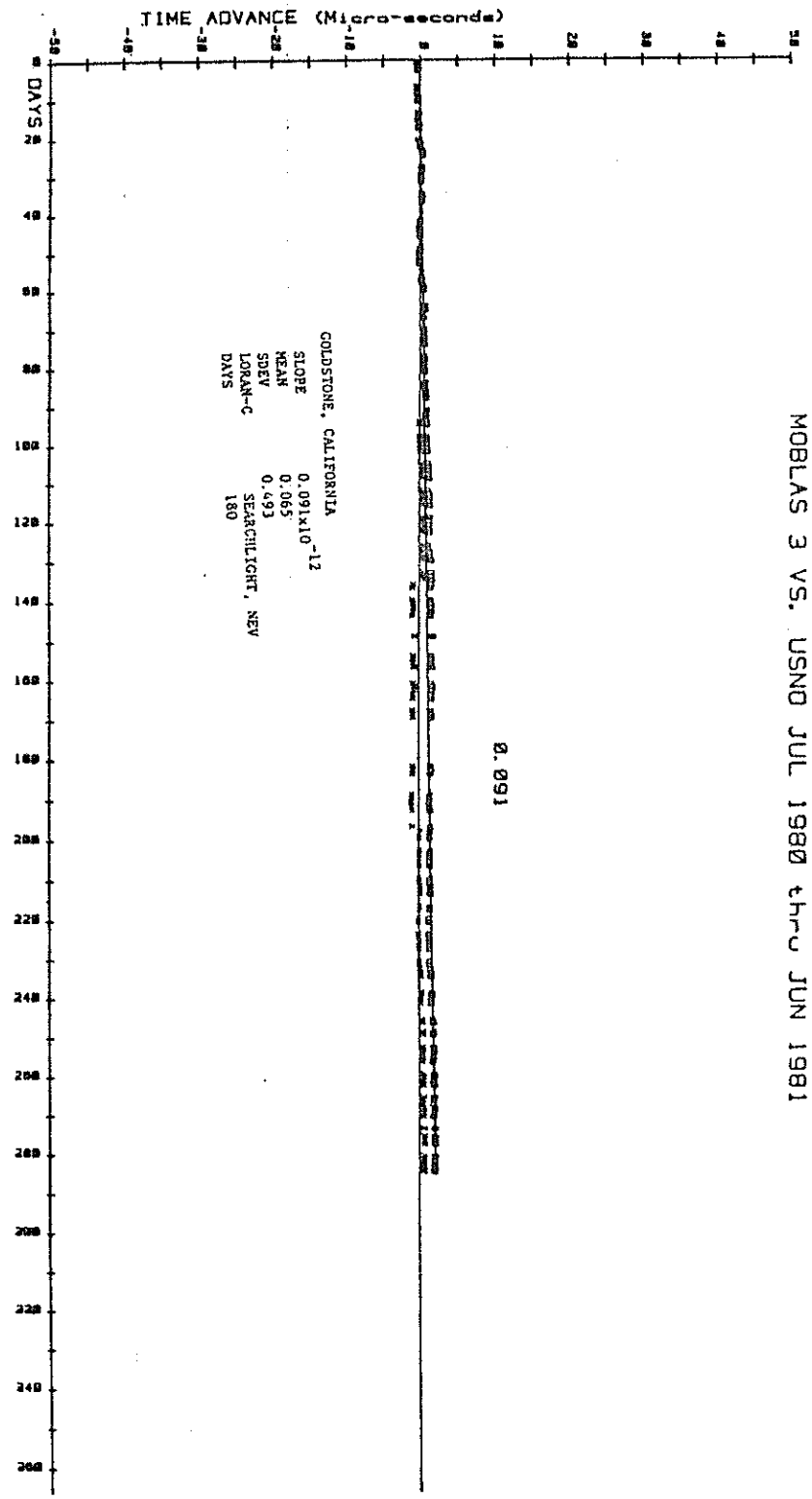
TIME ADVANCE (Micro-seconds)
DAYS
GOLDSTONE, CALIFORNIA
SLOPE 0.091x10-12
MEAN 0.065
SDEV 0.491
LORAN-C SEARCHLIGHT, NEV
DAYS 180
0.091
MOBLAS 3 VS. USNO JUL 1980 thru JUN 1981

Figure 1

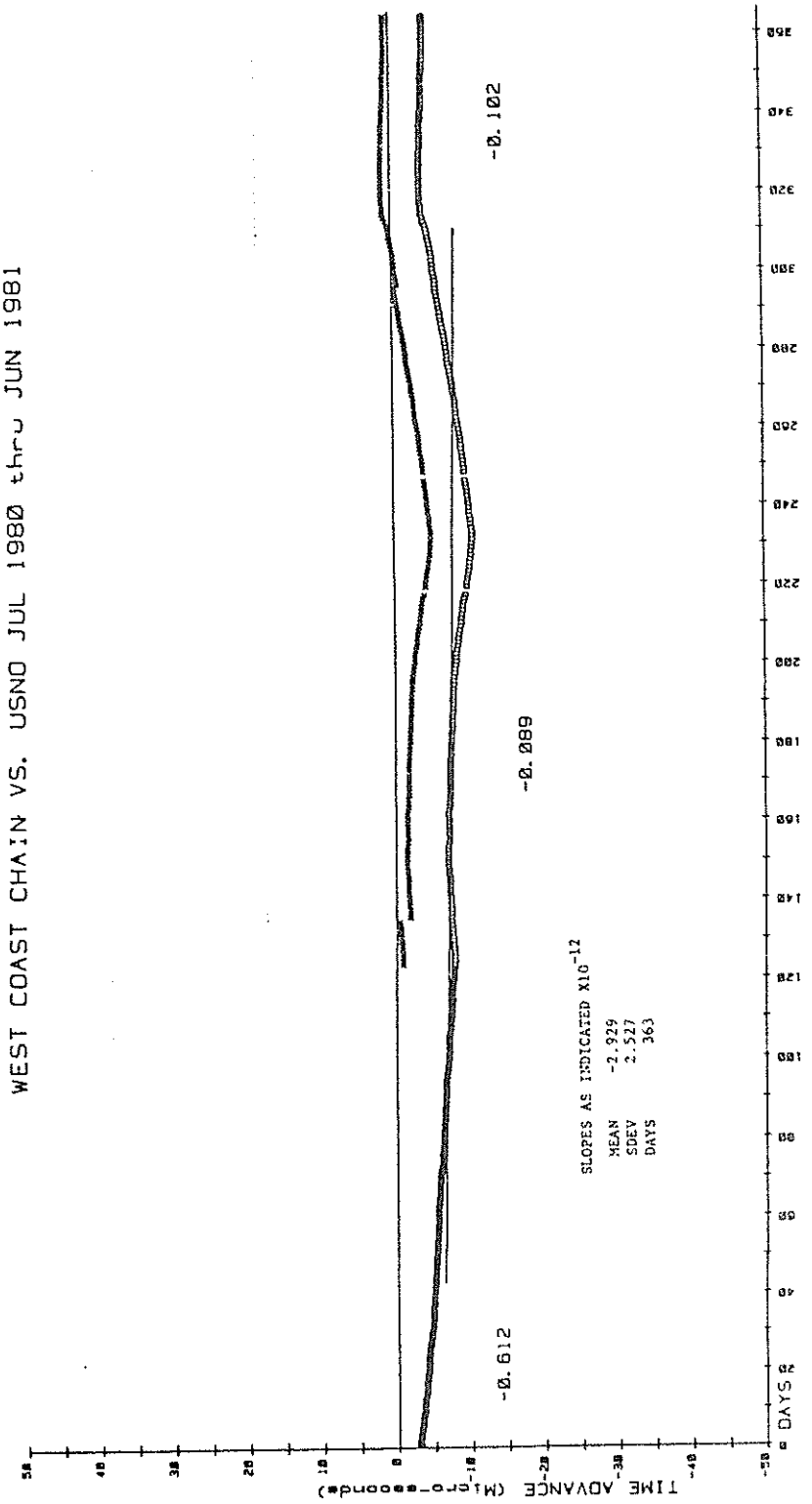
WEST COAST CHAIN VS. USNO JUL 1980 thru JUN 1981
TIME ADVANCE (Micro-seconds)
DAYS
-0.102
-0.089
-0.612
SLOPES AS INDICATED X10-12
MEAN -2.929
SDEV 2.527
DAYS 363

Figure 2

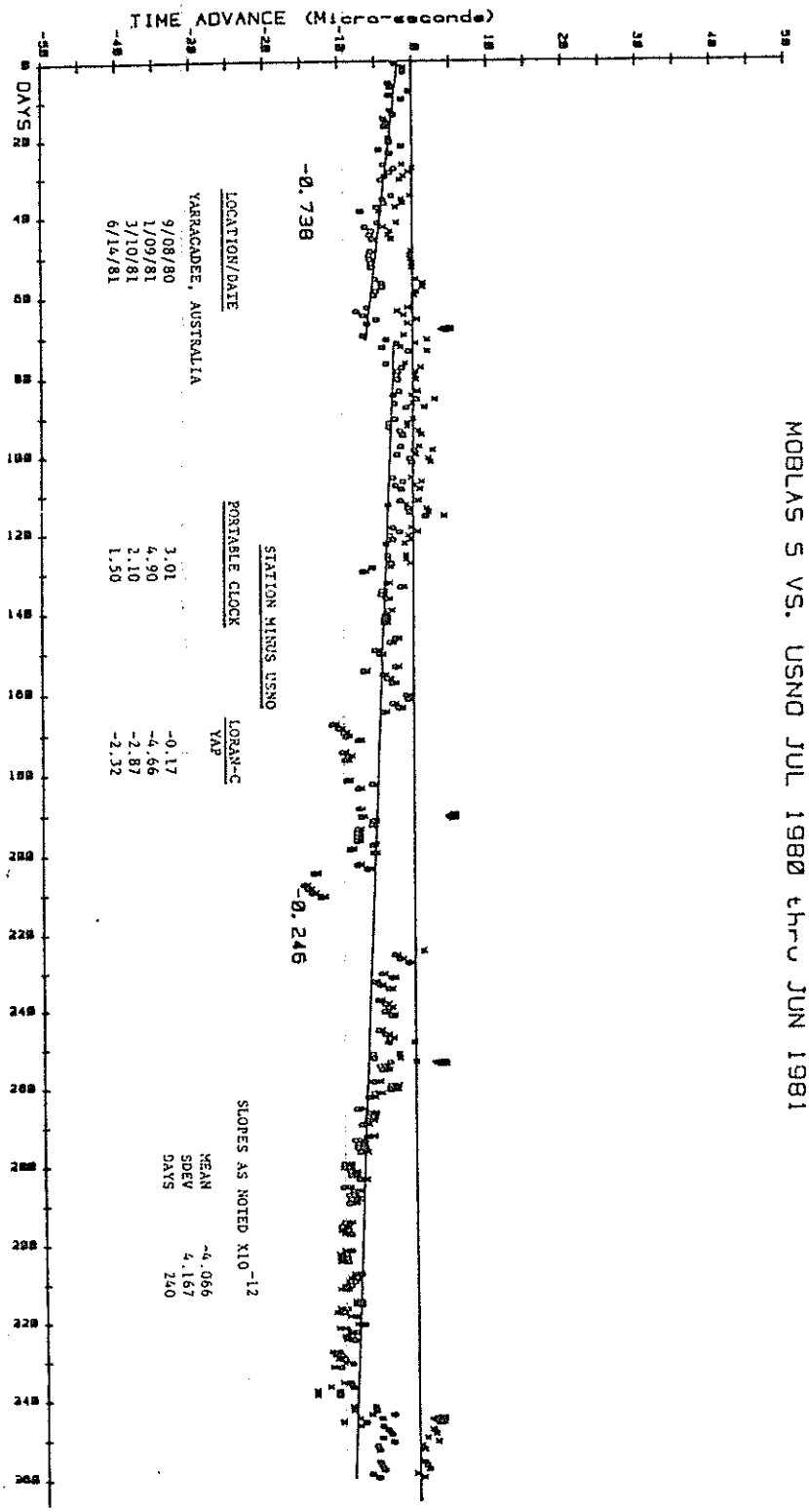
TIME ADVANCE (Micro-seconds)
DAYS
MOBLAS 5 VS. USNO JUL 1980 thru JUN 1981
-0.738
-0.246
STATION MINUS USNO
LOCATION/DATE
PORTABLE CLOCK
LORAN-C
YAP
YARRAGADEE, AUSTRALIA
9/08/80
1/09/81
3/10/81
6/14/81
3.01
4.90
2.10
1.50
-0.17
-4.66
-2.87
-2.32
SLOPES AS NOTED X10-12
MEAN -4.066
SDEV 4.167
DAYS 240

Figure 3

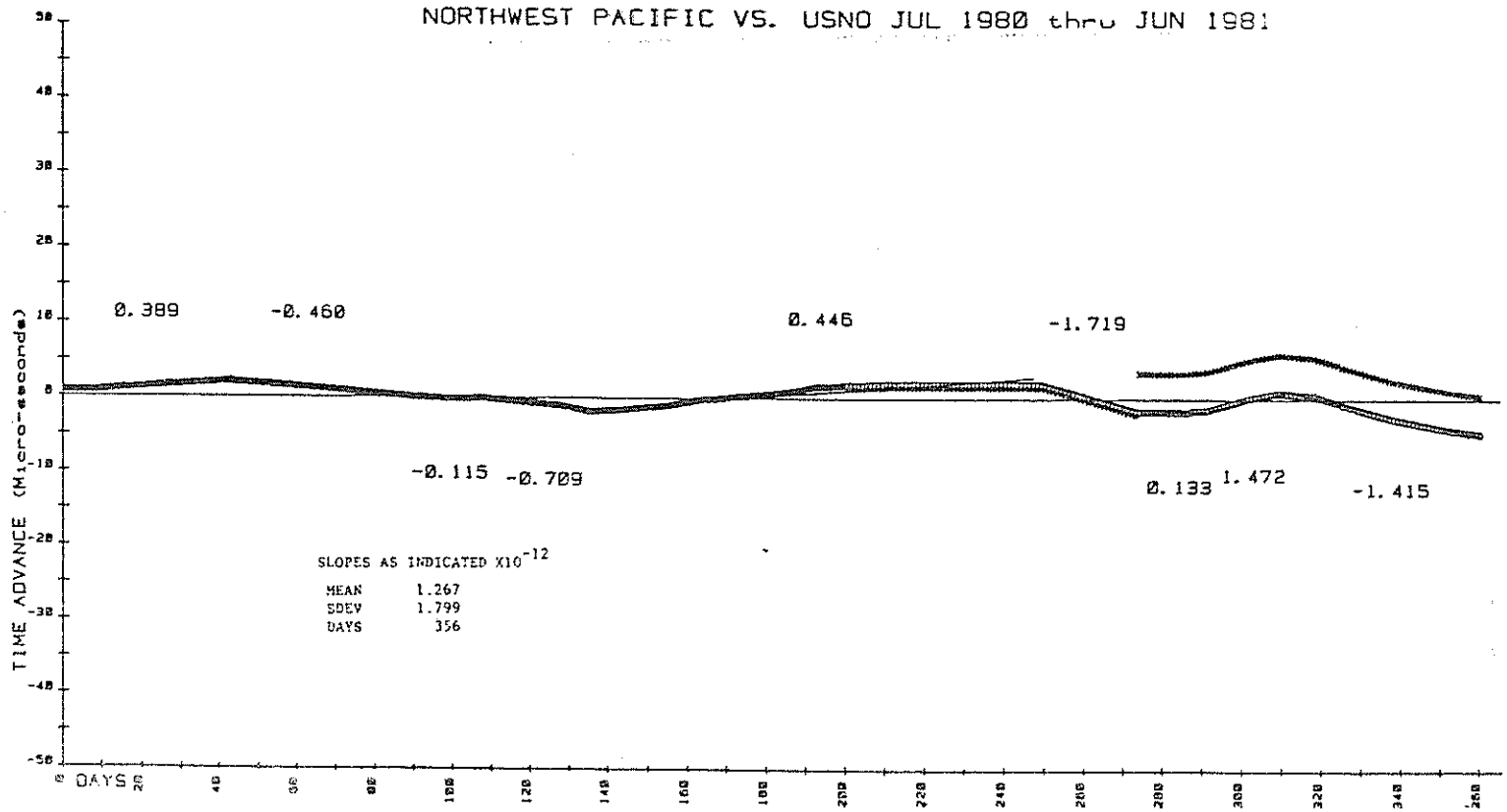
NORTHWEST PACIFIC VS. USNO JUL 1980 thru JUN 1981
TIME ADVANCE (Micro-seconds)
DAYS
0.389
-0.460
0.446
-1.719
-0.115
-0.709
0.133
1.472
-1.415
SLOPES AS INDICATED X10^-12
MEAN 1.267
SDEV 1.799
DAYS 356

Figure 4

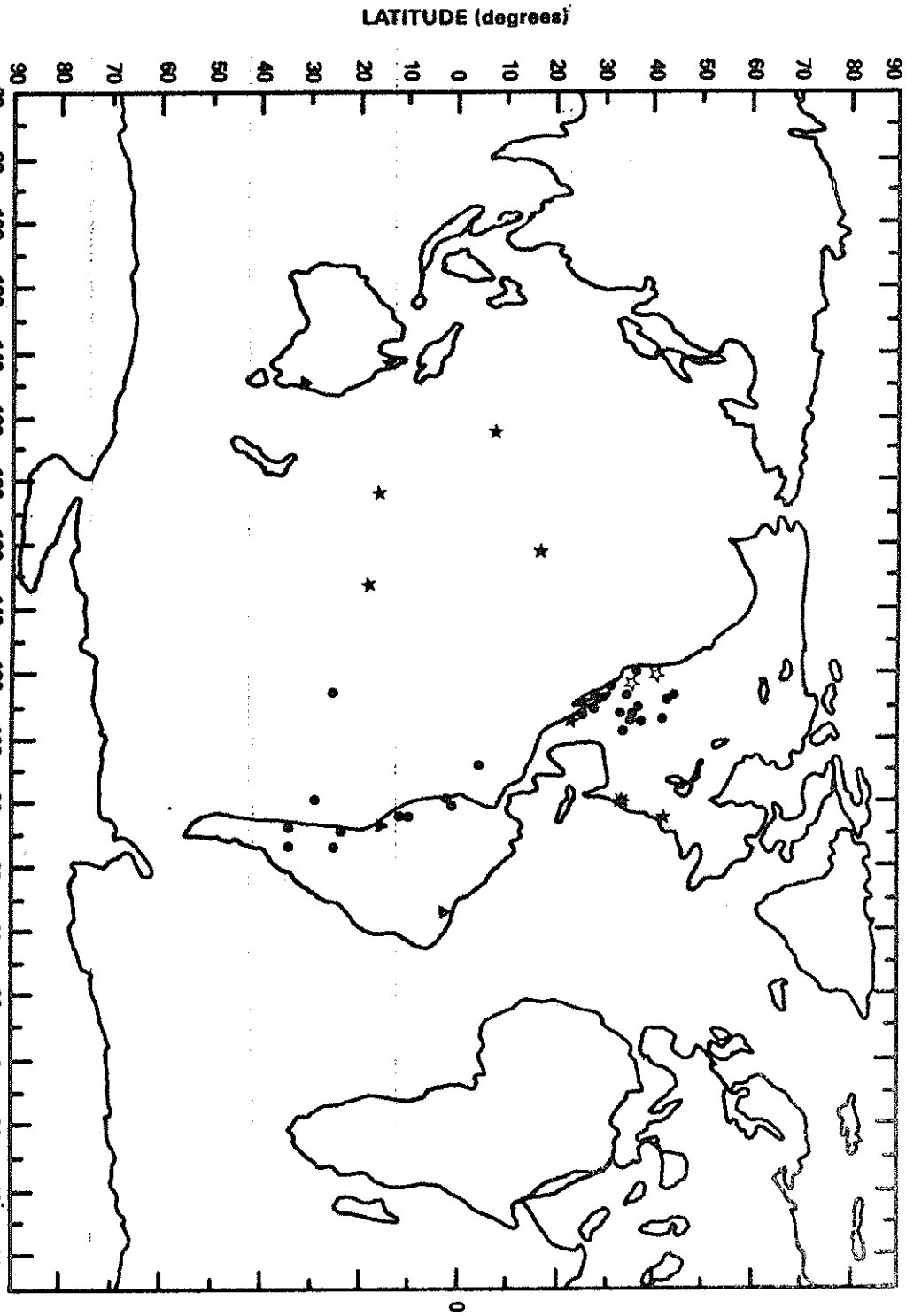
NASA-GSFC LASER TRACKING SITES 1980 - 1986
LATITUDE (degrees)
WEST LONGITUDE (degrees)
* STALAS
★ MOBLAS
● TLRS
☆ MOBLAS/TLRS
▲ SAO

Figure 5

TENTATIVE LASER DEPLOYMENT SCHEDULE

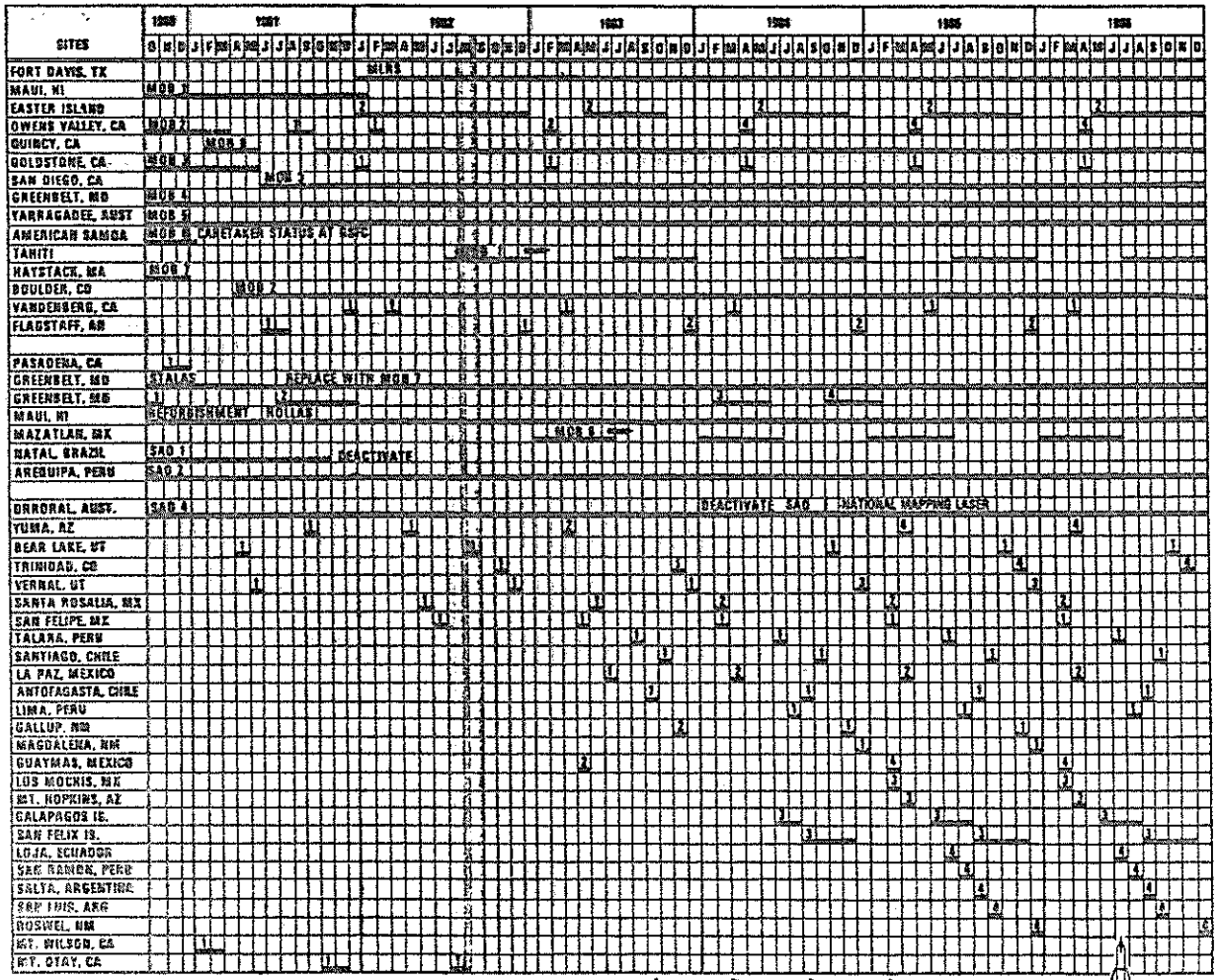

LASER NETWORK MANAGER

LASER PROJECT MANAGER

CRUSTAL DYNAMICS PROJECT MANAGER

Figure 6

NAVSTAR GPS
STATION SYNCHRONIZATION
BY
TIME TRANSFER

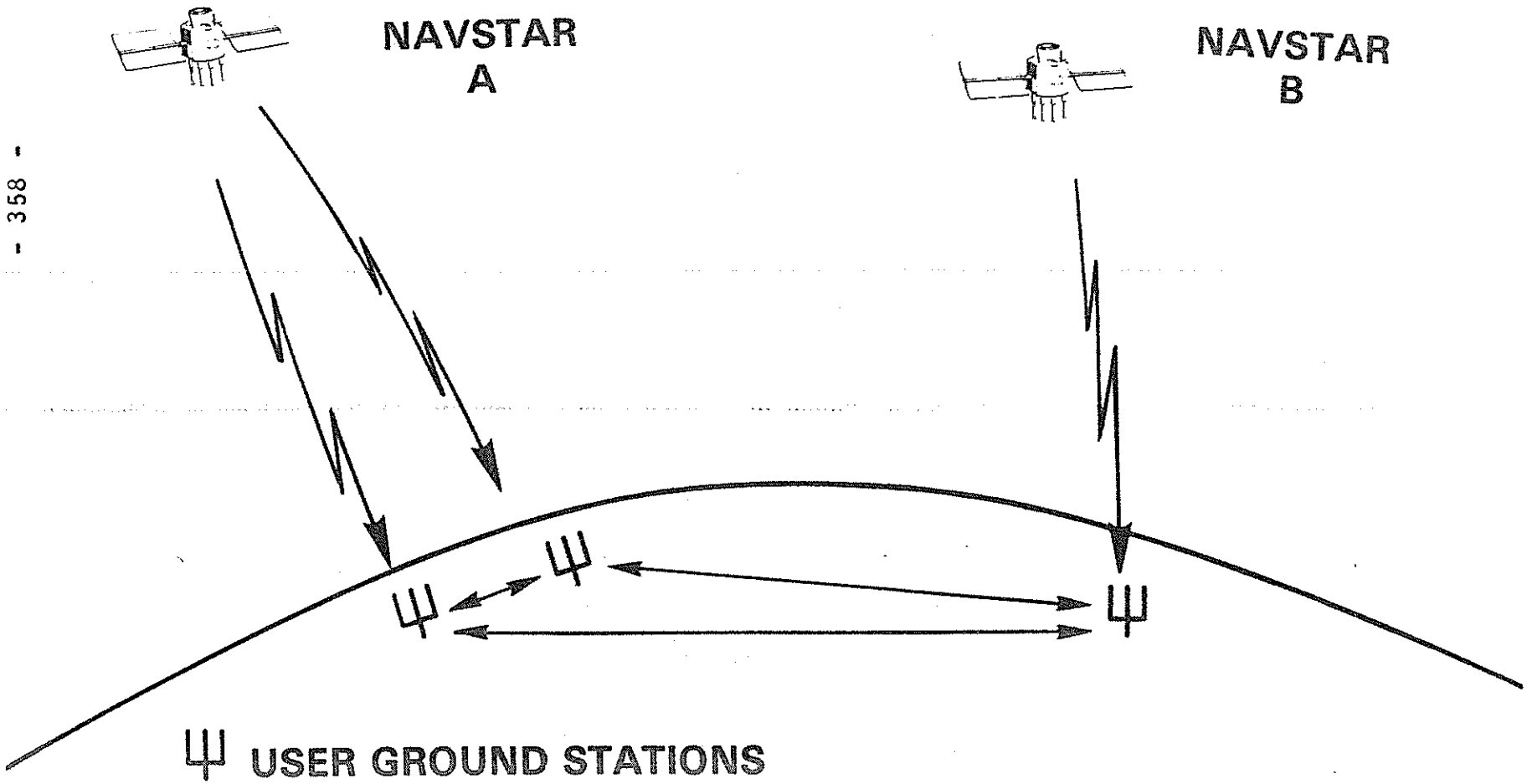

NAVSTAR

Global Positioning System

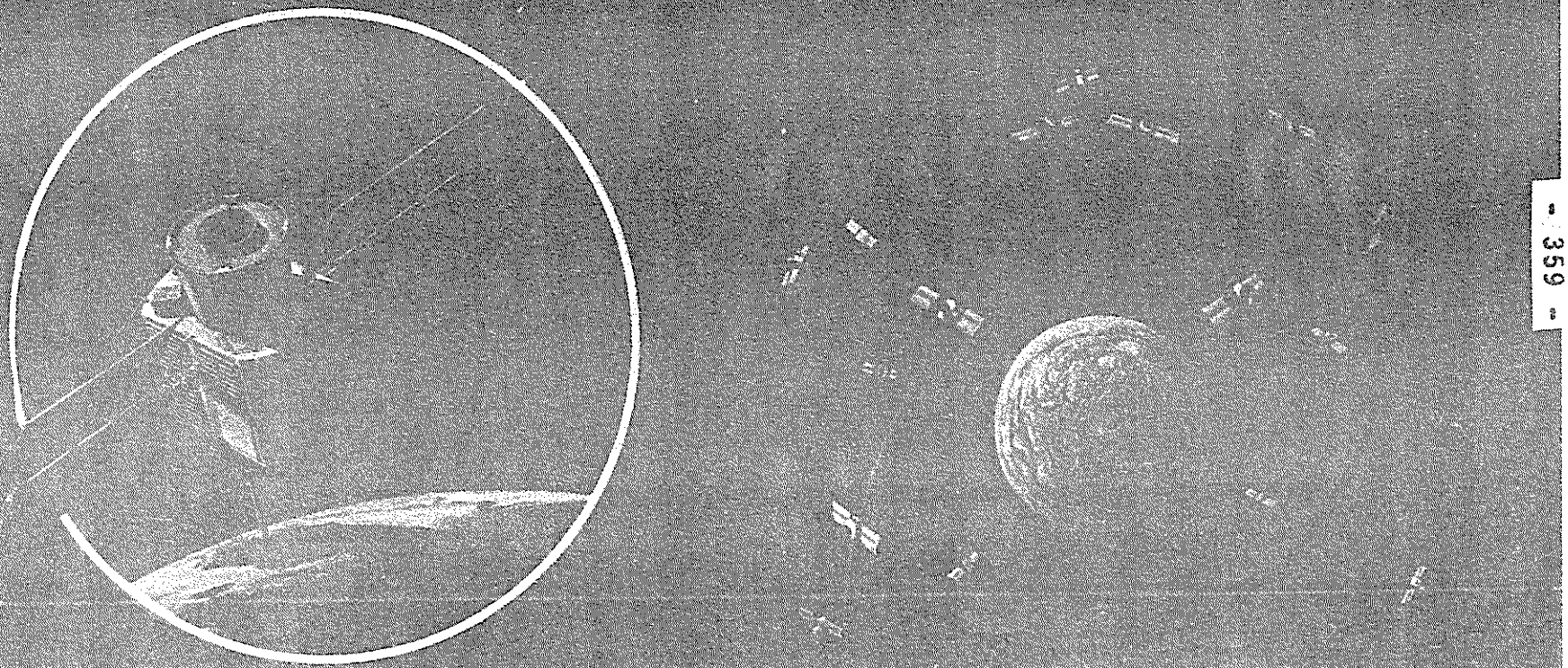

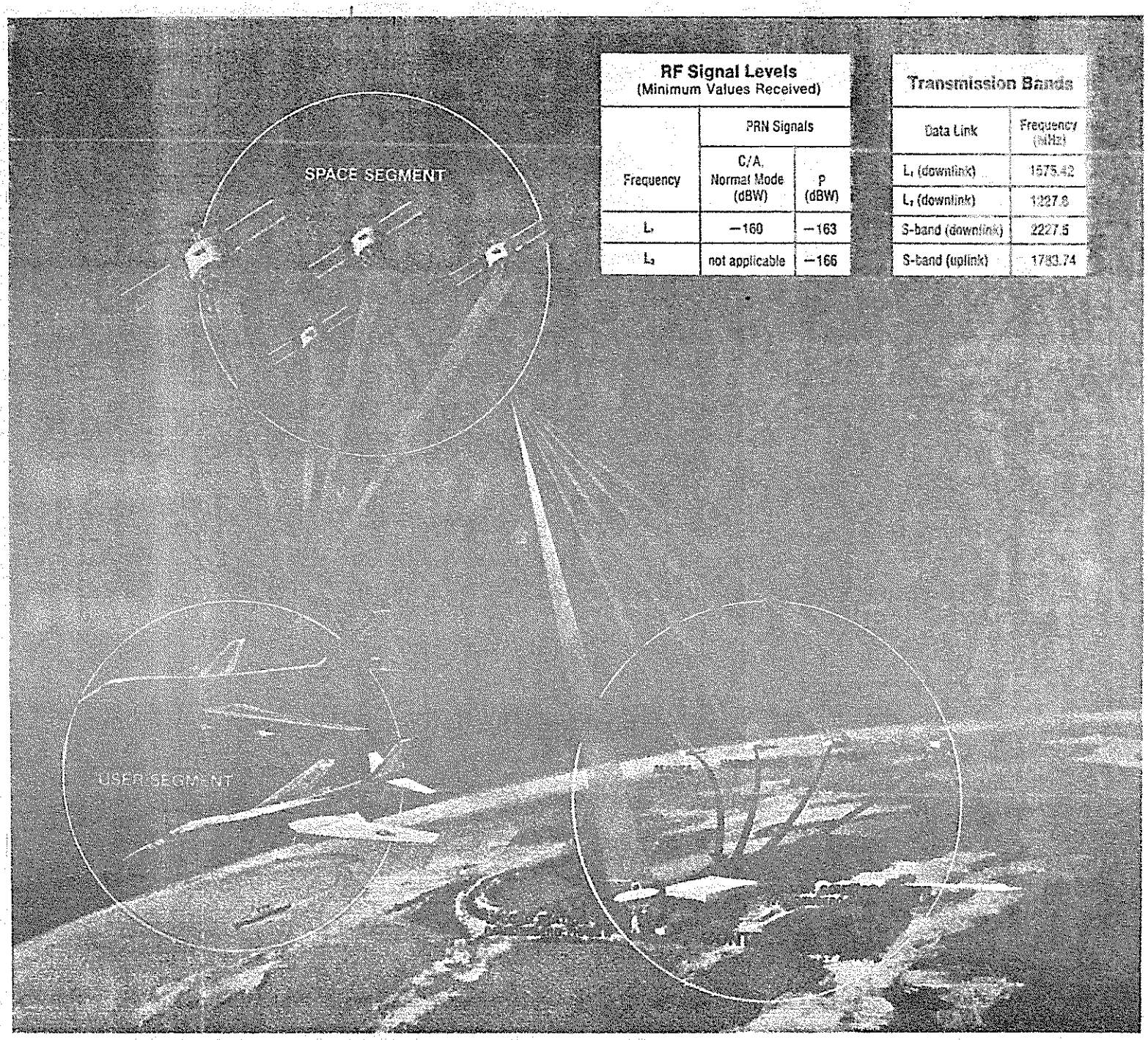

RF Signal Levels
(Minimum Values Received)

Frequency	PRN Signals	
	C/A, Normal Mode (dBW)	P (dBW)
L_1	−160	−163
L_2	not applicable	−166

Transmission Bands

Data Link	Frequency (MHz)
L_1 (downlink)	1575.42
L_2 (downlink)	1227.6
S-band (downlink)	2227.5
S-band (uplink)	1783.74

Figure 9

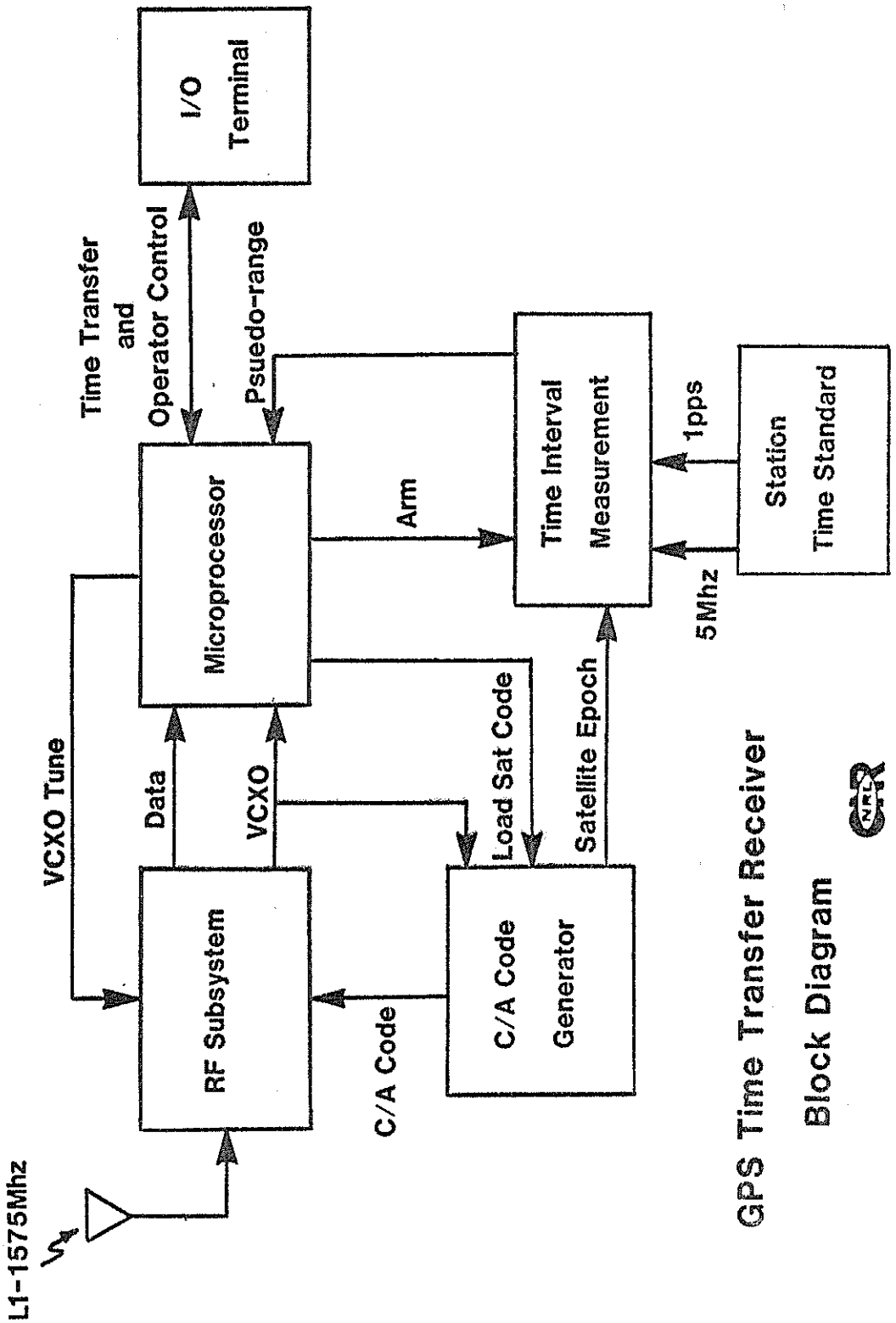
I/O Terminal
Time Transfer and Operator Control
Psuedo-range
Microprocessor
Arm
Time Interval Measurement
1pps
Station Time Standard
5Mhz
VCXO Tune
Data
VCXO
Load Sat Code
Satellite Epoch
RF Subsystem
C/A Code Generator
C/A Code
L1-1575Mhz
GPS Time Transfer Receiver
Block Diagram
NRL

Figure 10

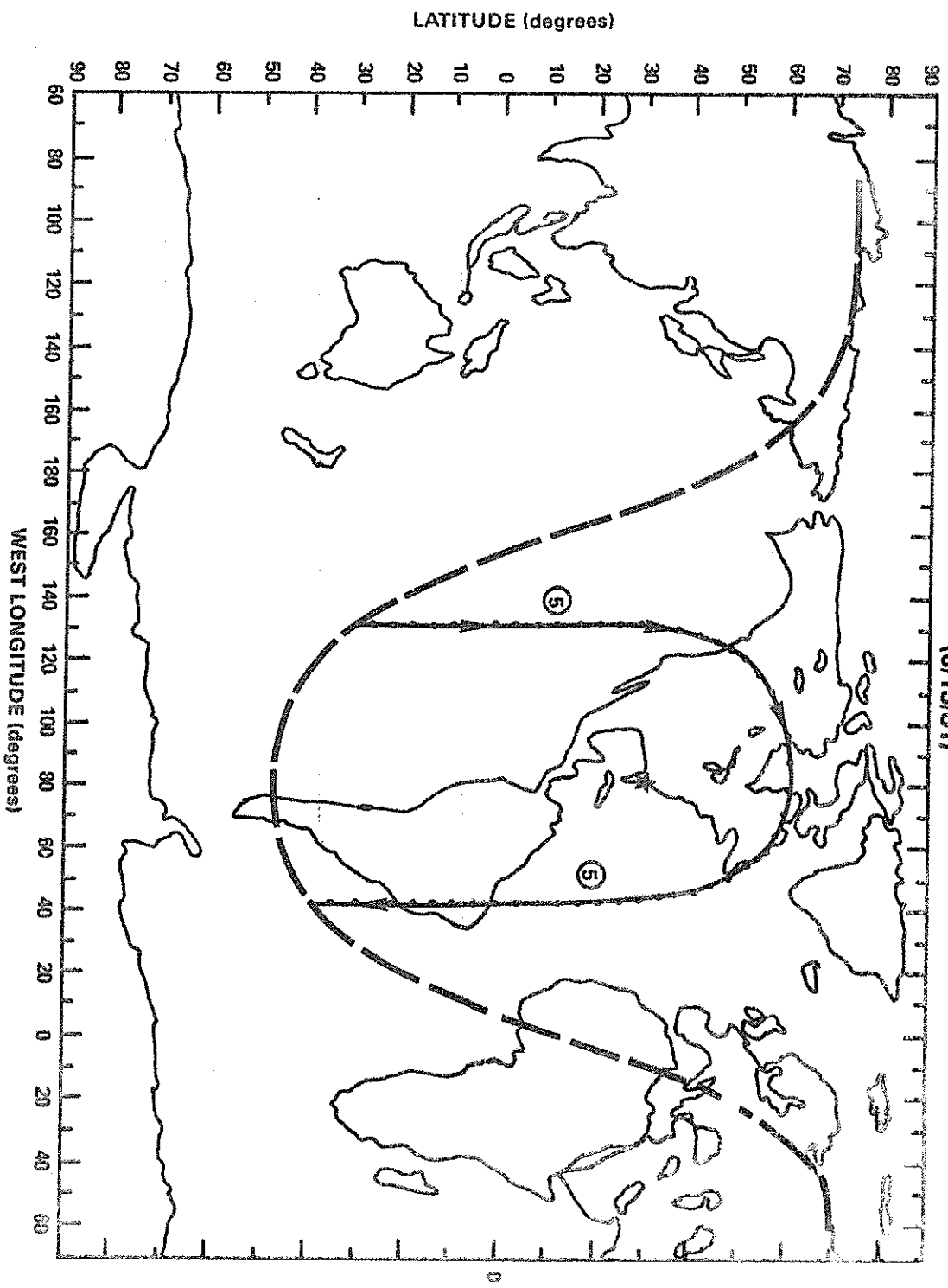
GPS NAVSTAR
MILA
GROUND TRACK
(6/15/81)
LATITUDE (degrees)
WEST LONGITUDE (degrees)
5
5

Figure 11

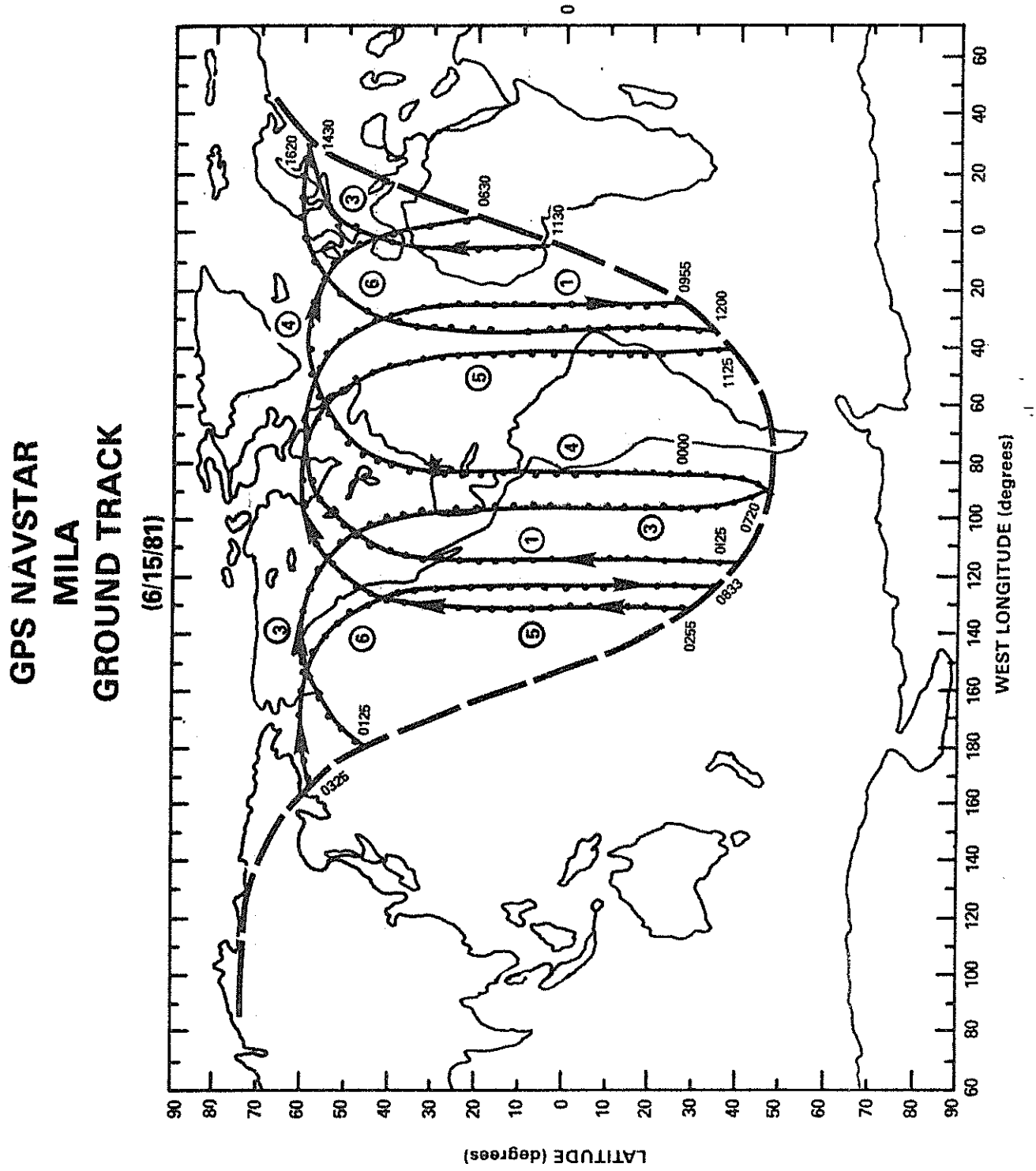
GPS NAVSTAR
MILA
GROUND TRACK
(6/15/81)
LATITUDE (degrees)
WEST LONGITUDE (degrees)
0
1620
1430
0630
1130
0955
1200
1125
0000
0720
0125
0833
0255
0125
0325

Figure 12

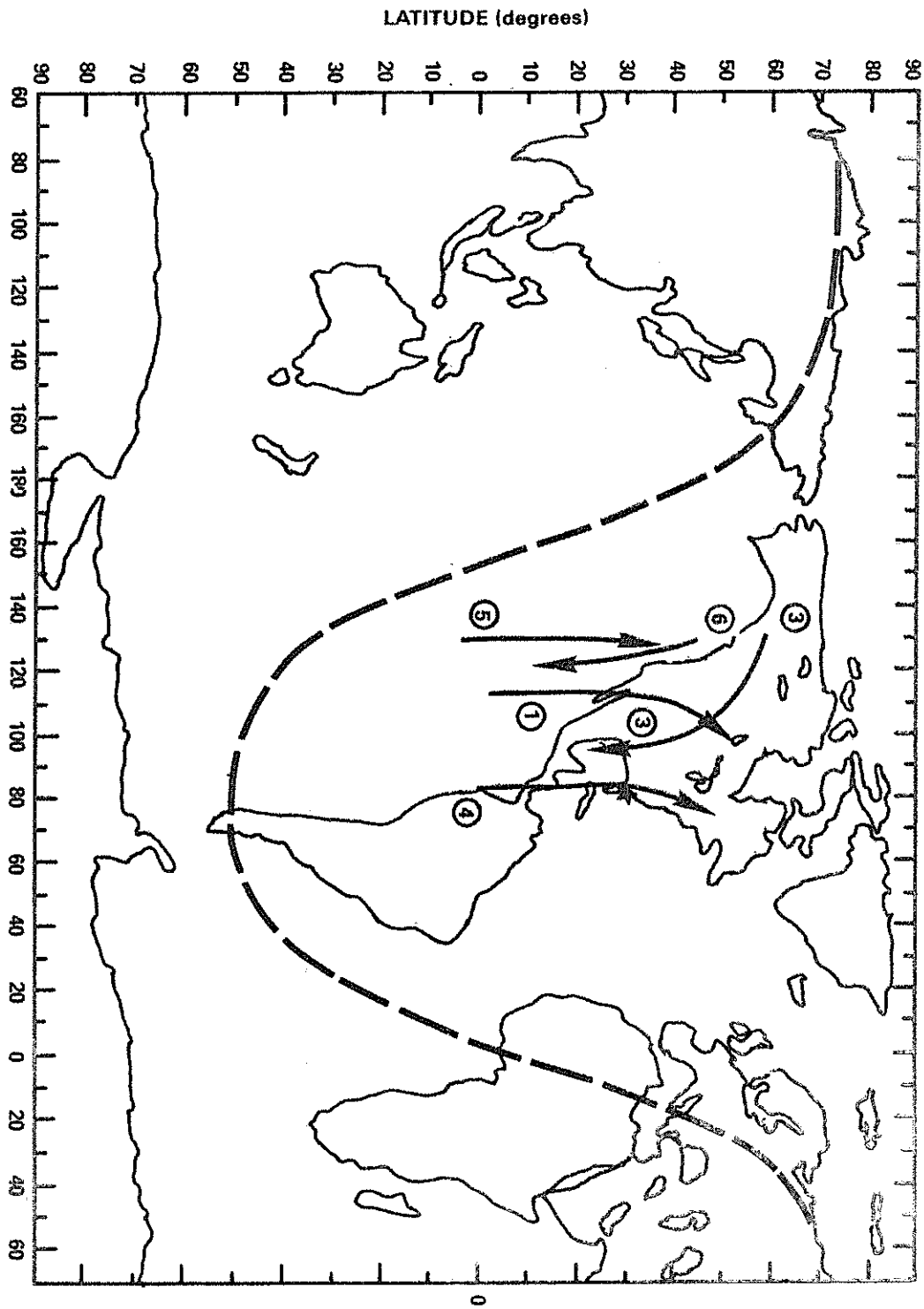
GPS NAVSTAR
MILA
GROUND TRACK
(6/15/81)
LATITUDE (degrees)
WEST LONGITUDE (degrees)
90 80 70 60 50 40 30 20 10 0 10 20 30 40 50 60 70 80 90
60 80 100 120 140 160 180 160 140 120 100 80 60 40 20 0 20 40 60
0
1
2
3
4
5
6

Figure 13

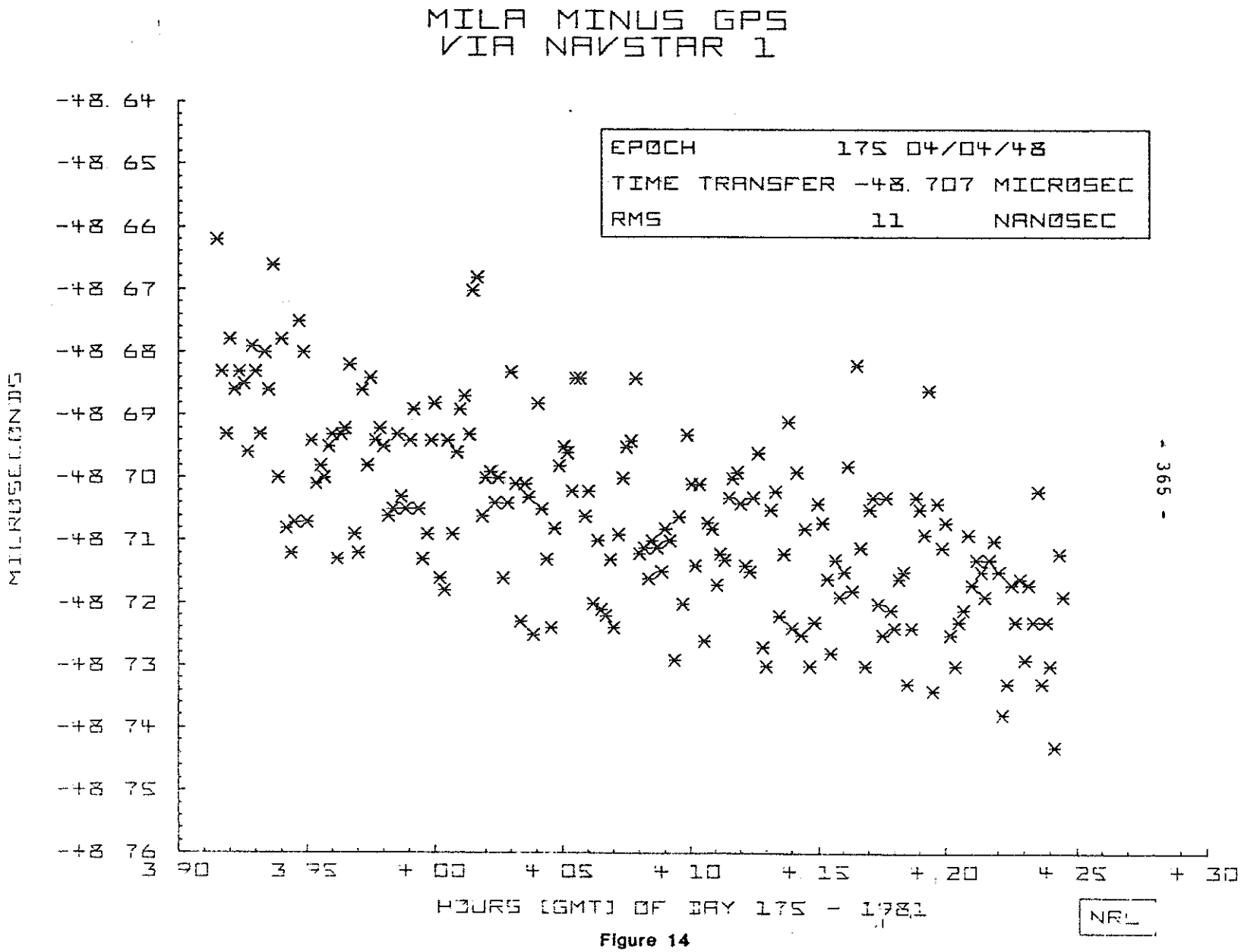

Figure 14

- 365 -

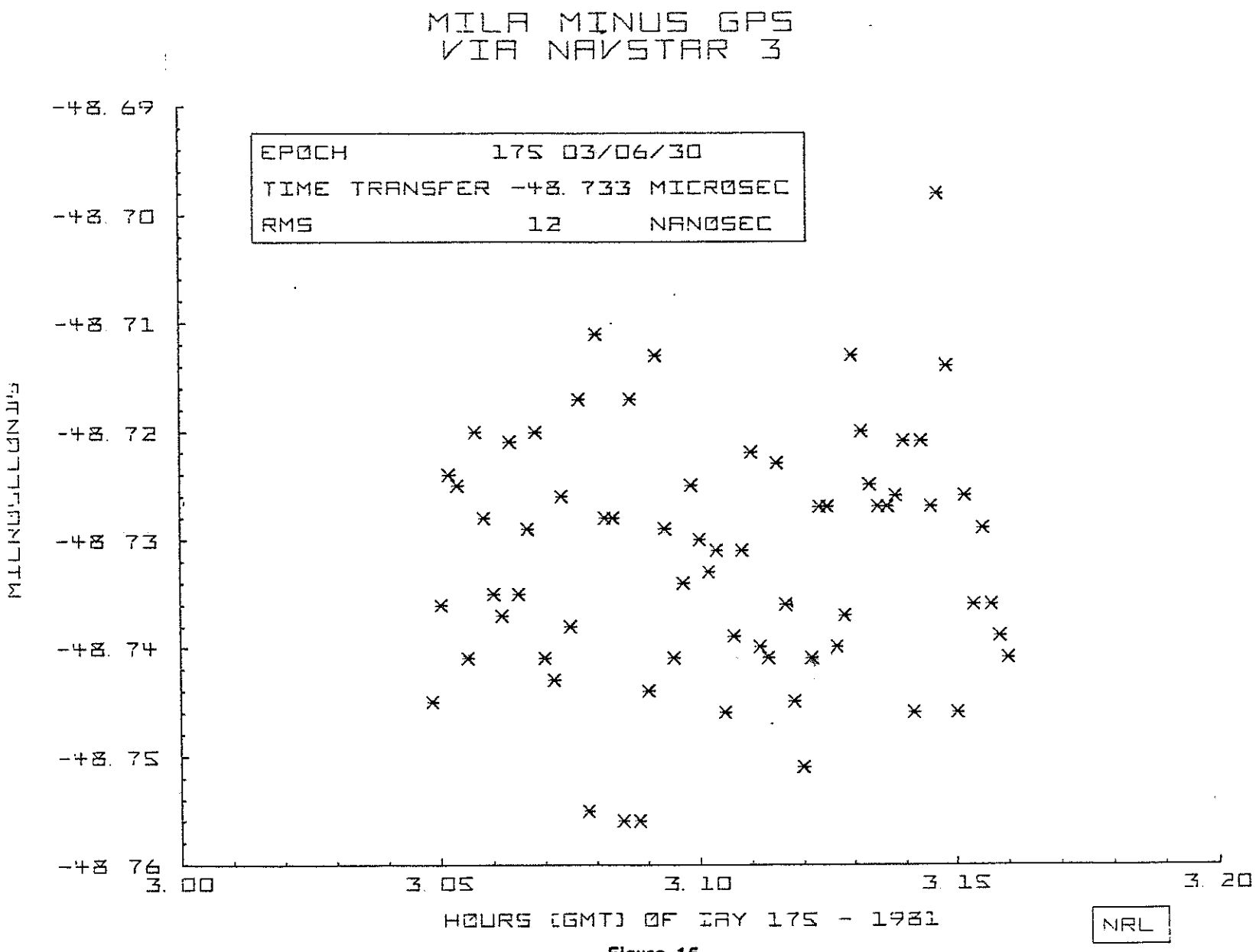
MILA MINUS GPS
VIA NAVSTAR 3
EPOCH 175 03/06/30
TIME TRANSFER -48.733 MICROSEC
RMS 12 NANOSEC
-48.69
-48.70
-48.71
-48.72
-48.73
-48.74
-48.75
-48.76
MICROSECONDS
3.00
3.05
3.10
3.15
3.20
HOURS (GMT) OF DAY 175 - 1981
NRL

Figure 15

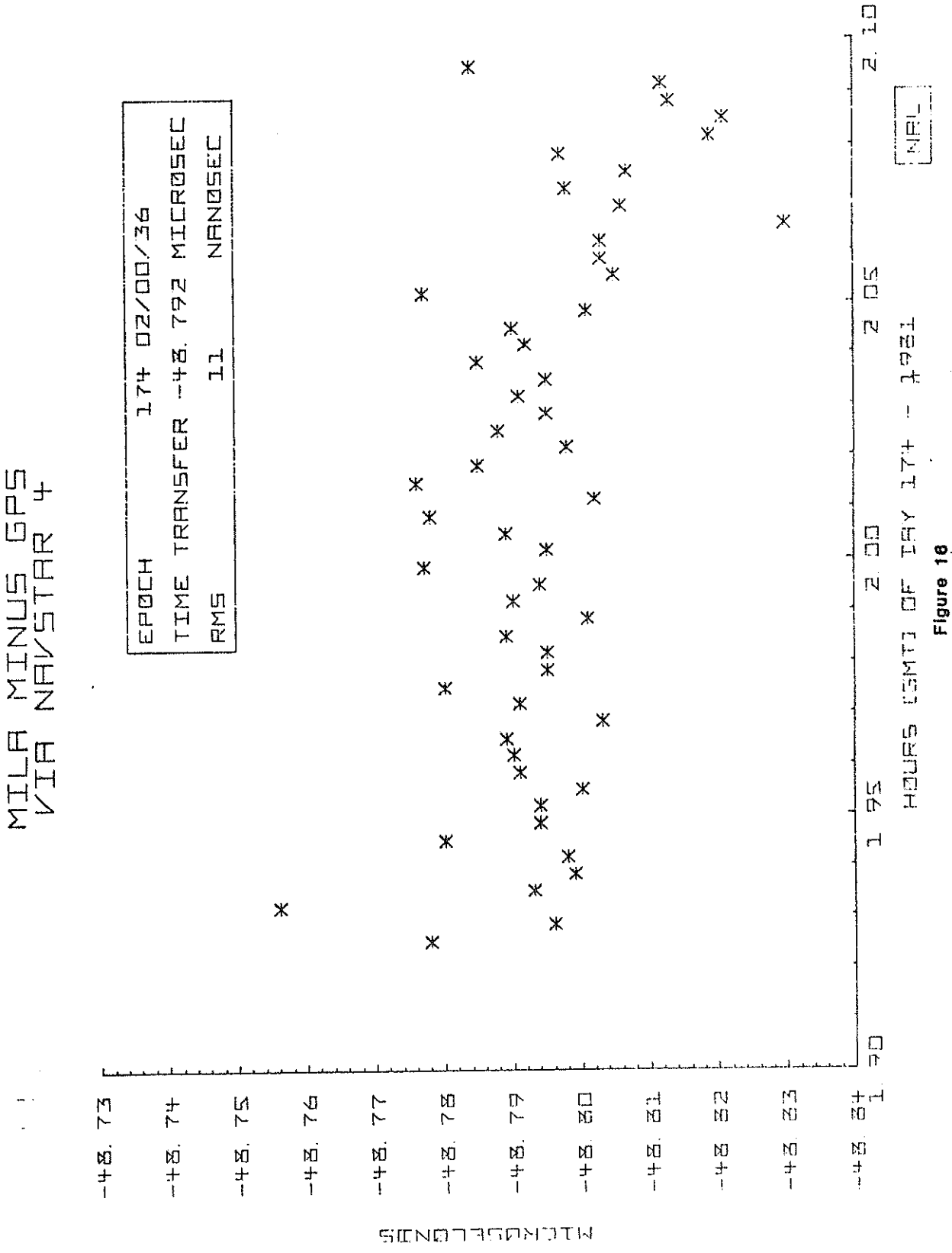
MILA MINUS GPS
VIA NAVSTAR 4
EPOCH 174 02/00/36
TIME TRANSFER -48.792 MICROSEC
RMS 11 NANOSEC
MICROSECONDS
-48.73
-48.74
-48.75
-48.76
-48.77
-48.78
-48.79
-48.80
-48.81
-48.82
-48.83
-48.84
0
1.95
2.00
2.05
2.10
HOURS GMT OF DAY 174 - 1981
NRL

Figure 16

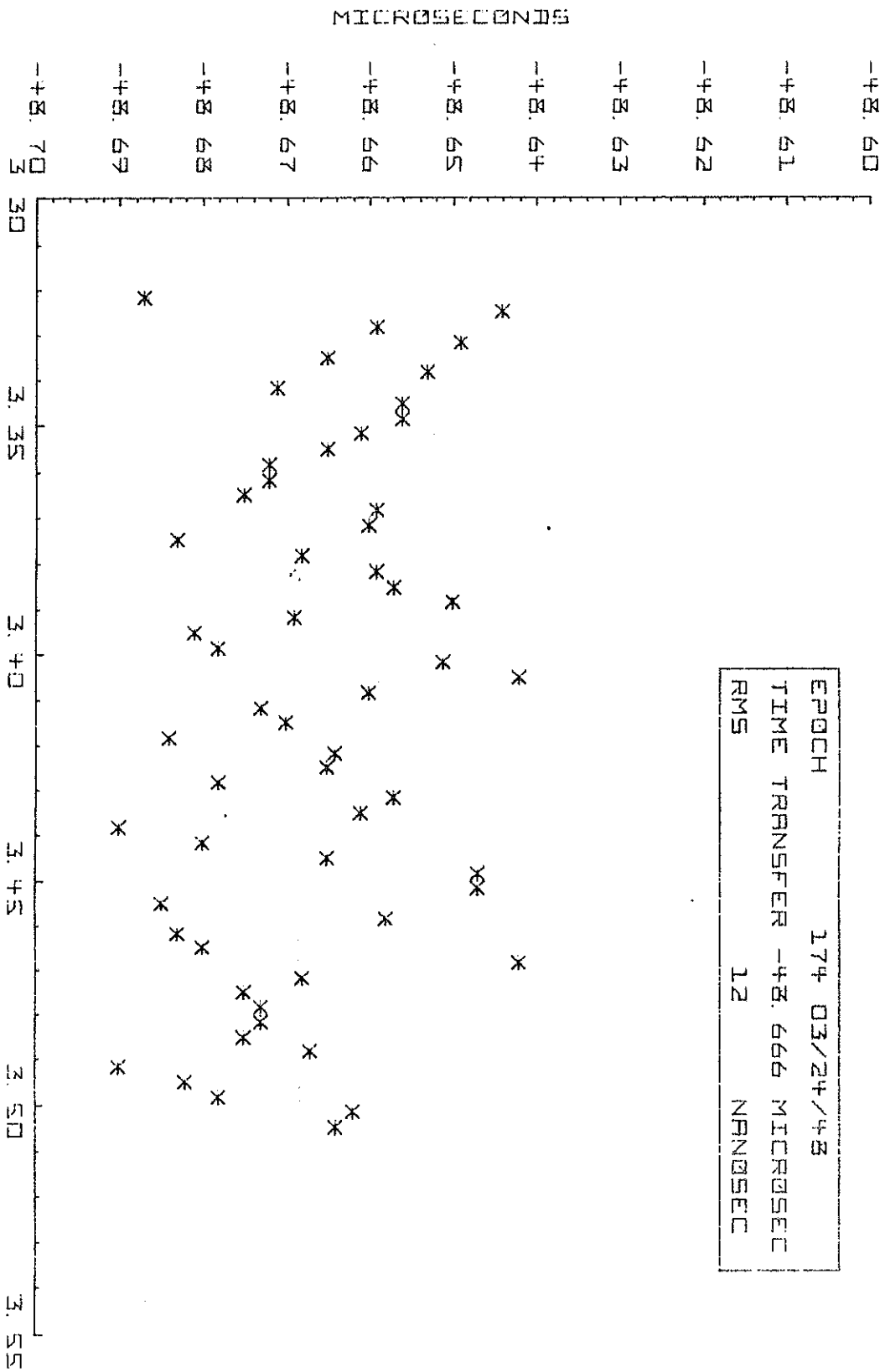
MILA MINUS GPS
VIA NAVSTAR 5
EPOCH 174 03/24/43
TIME TRANSFER -43.666 MICROSEC
RMS 12 NANOSEC
MICROSECONDS
-43.60
-43.61
-43.62
-43.63
-43.64
-43.65
-43.66
-43.67
-43.68
-43.69
-43.70
3.30
3.35
3.40
3.45
3.50
3.55
HOURS GMT OF DAY 174 - 1981
NRL

Figure 17

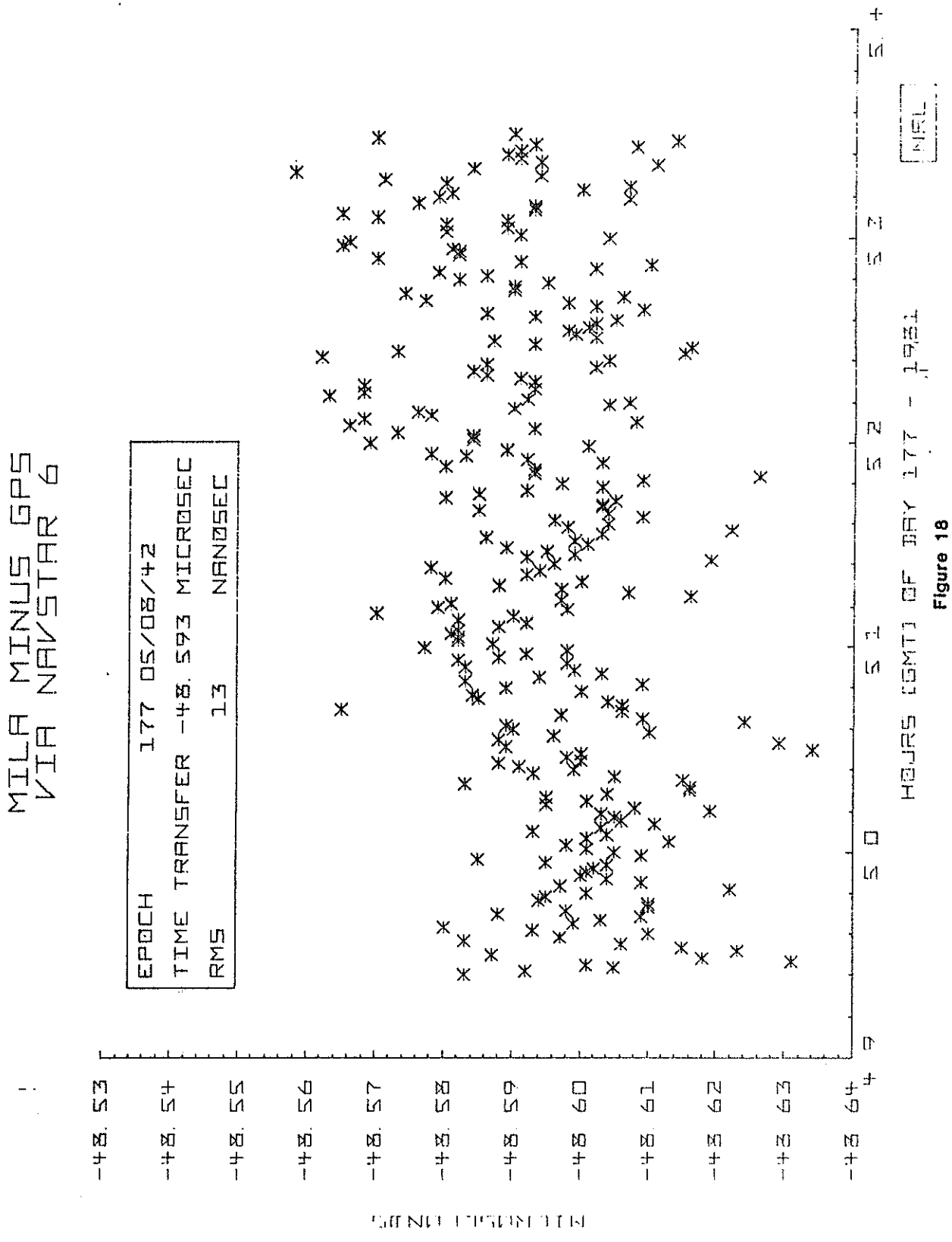
MILA MINUS GPS
VIA NAVSTAR 6
EPOCH 177 05/08/42
TIME TRANSFER -48.593 MICROSEC
RMS 13 NANOSEC
HOURS GMT OF DAY 177 - 1981
NBS

Figure 18

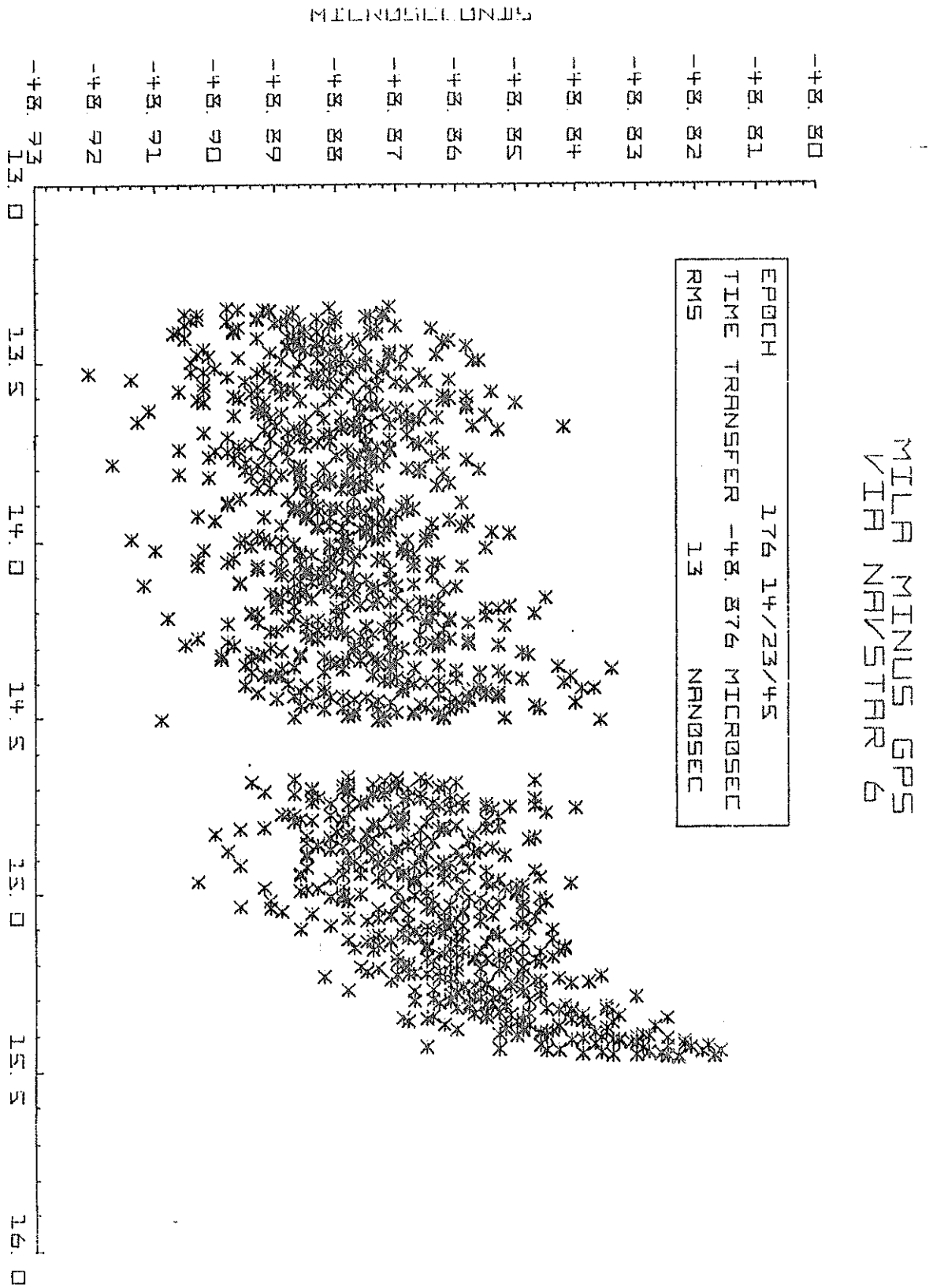
MILA MINUS GPS
VIA NAVSTAR 6
EPOCH 176 14/23/45
TIME TRANSFER -48.876 MICROSEC
RMS 13 NANOSEC
MICROSECONDS
-48.80
-48.81
-48.82
-48.83
-48.84
-48.85
-48.86
-48.87
-48.88
-48.89
-48.90
-48.91
-48.92
13.0
13.5
14.0
14.5
15.0
15.5
16.0
HOURS (GMT) OF DAY 176 - 1985
NRL

Figure 19

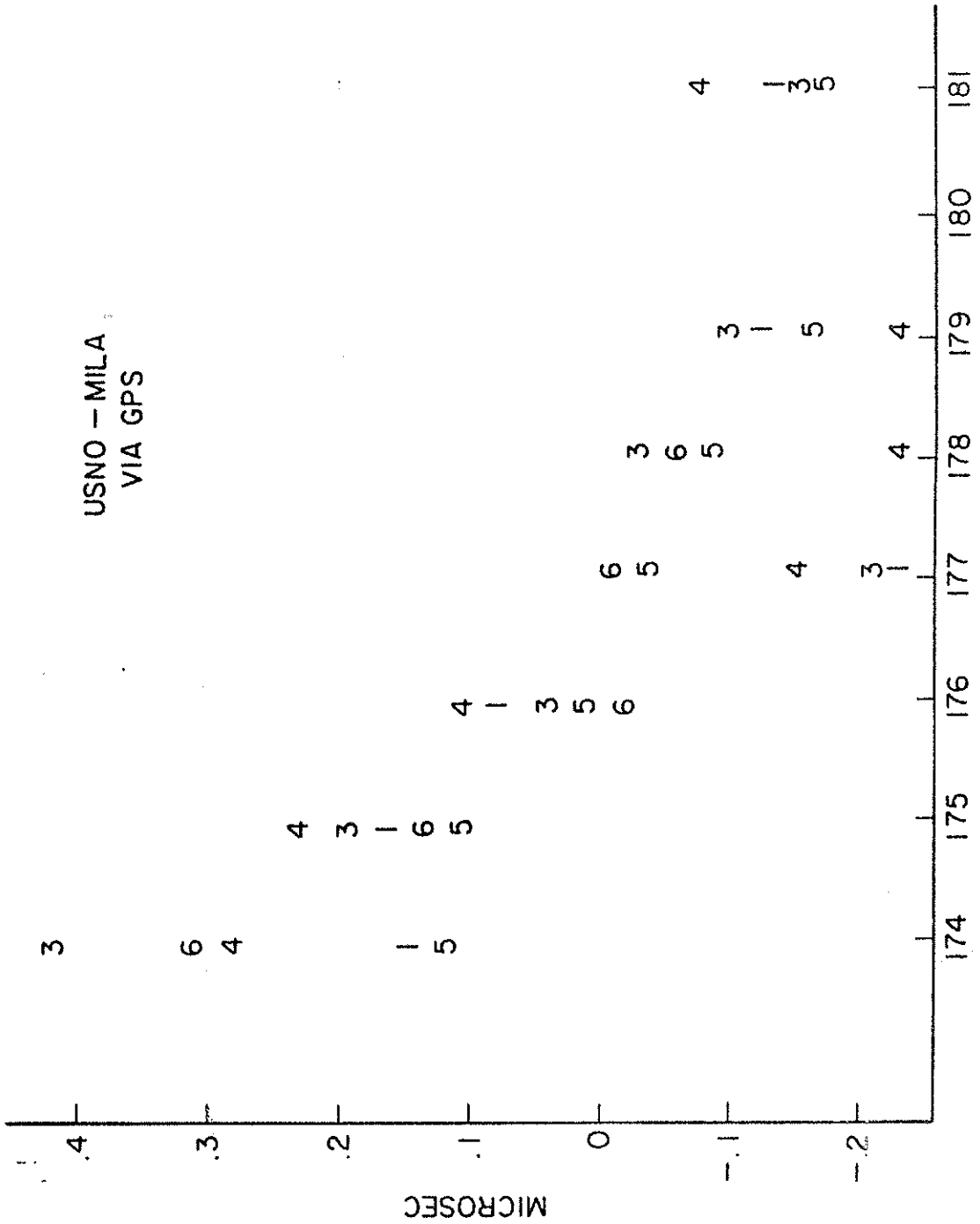
USNO – MILA
VIA GPS
MICROSEC
.4
.3
.2
.1
0
-.1
-.2
174
175
176
177
178
179
180
181
DAY (1981)

Figure 20

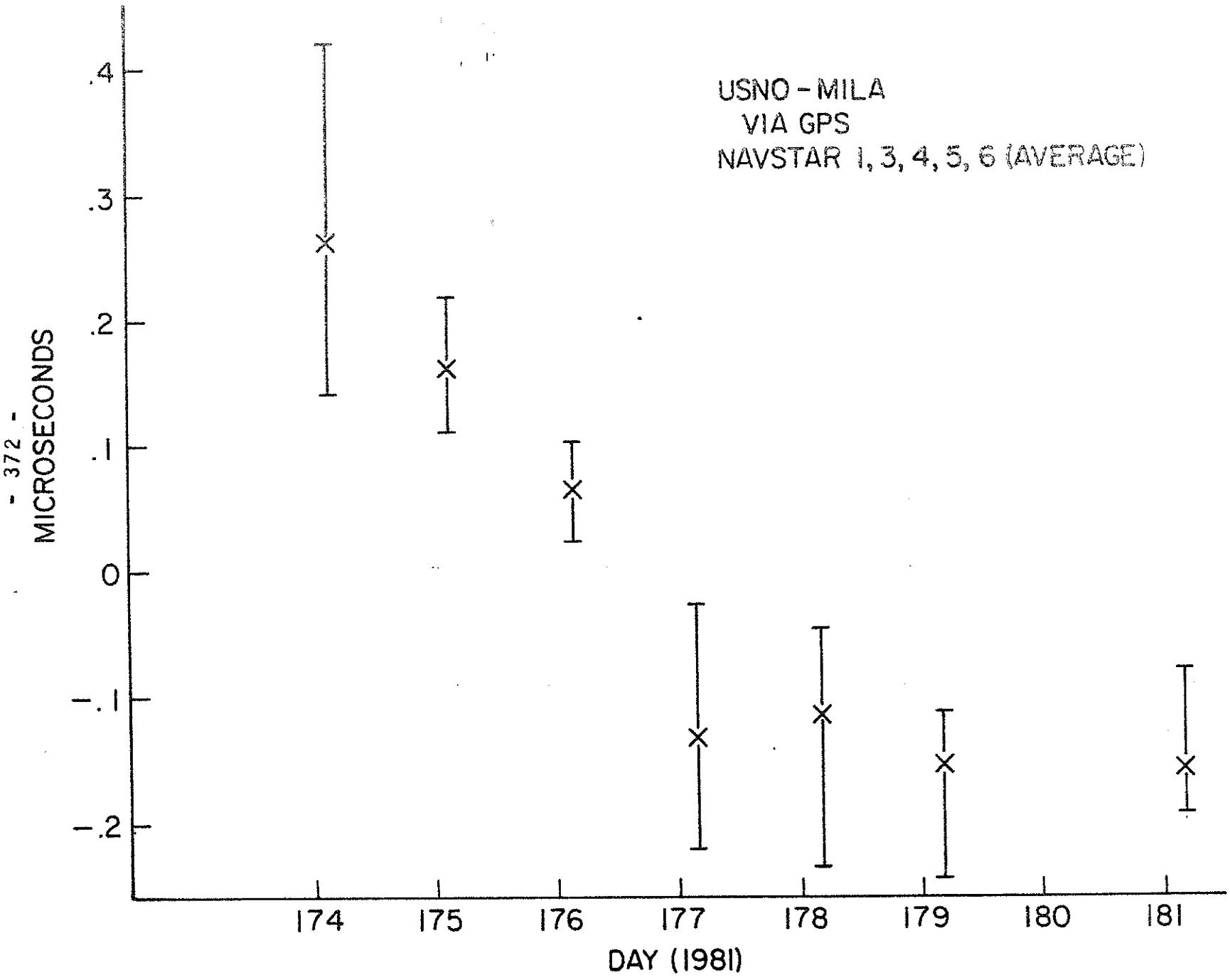
USNO - MILA
VIA GPS
NAVSTAR 1, 3, 4, 5, 6 (AVERAGE)
- 372 -
MICROSECONDS
.4
.3
.2
.1
0
-.1
-.2
174
175
176
177
178
179
180
181
DAY (1981)

Figure 21

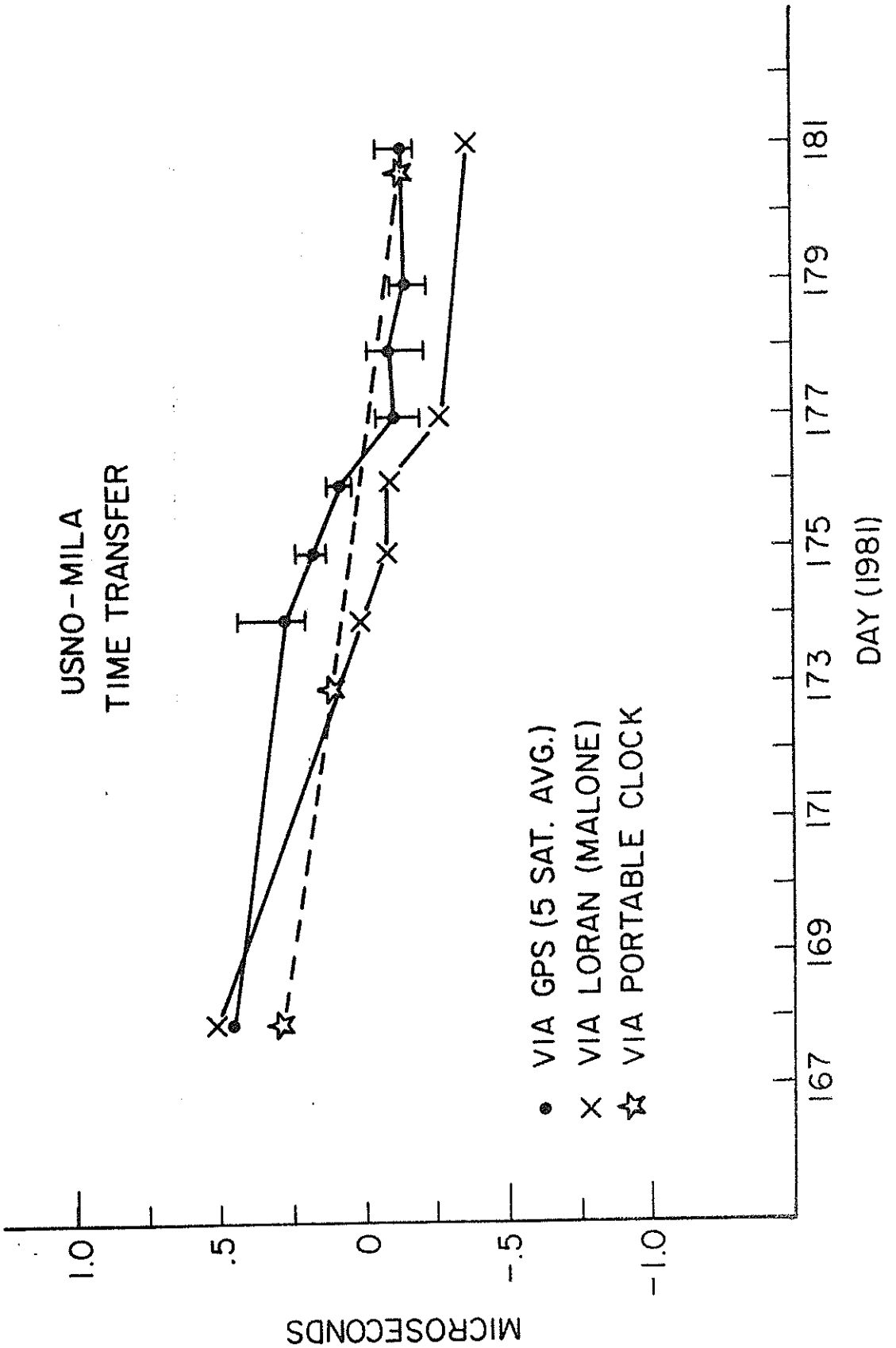
USNO-MILA
TIME TRANSFER
VIA GPS (5 SAT. AVG.)
VIA LORAN (MALONE)
VIA PORTABLE CLOCK
MICROSECONDS
1.0
.5
0
-.5
-1.0
167
169
171
173
175
177
179
181
DAY (1981)

Figure 22

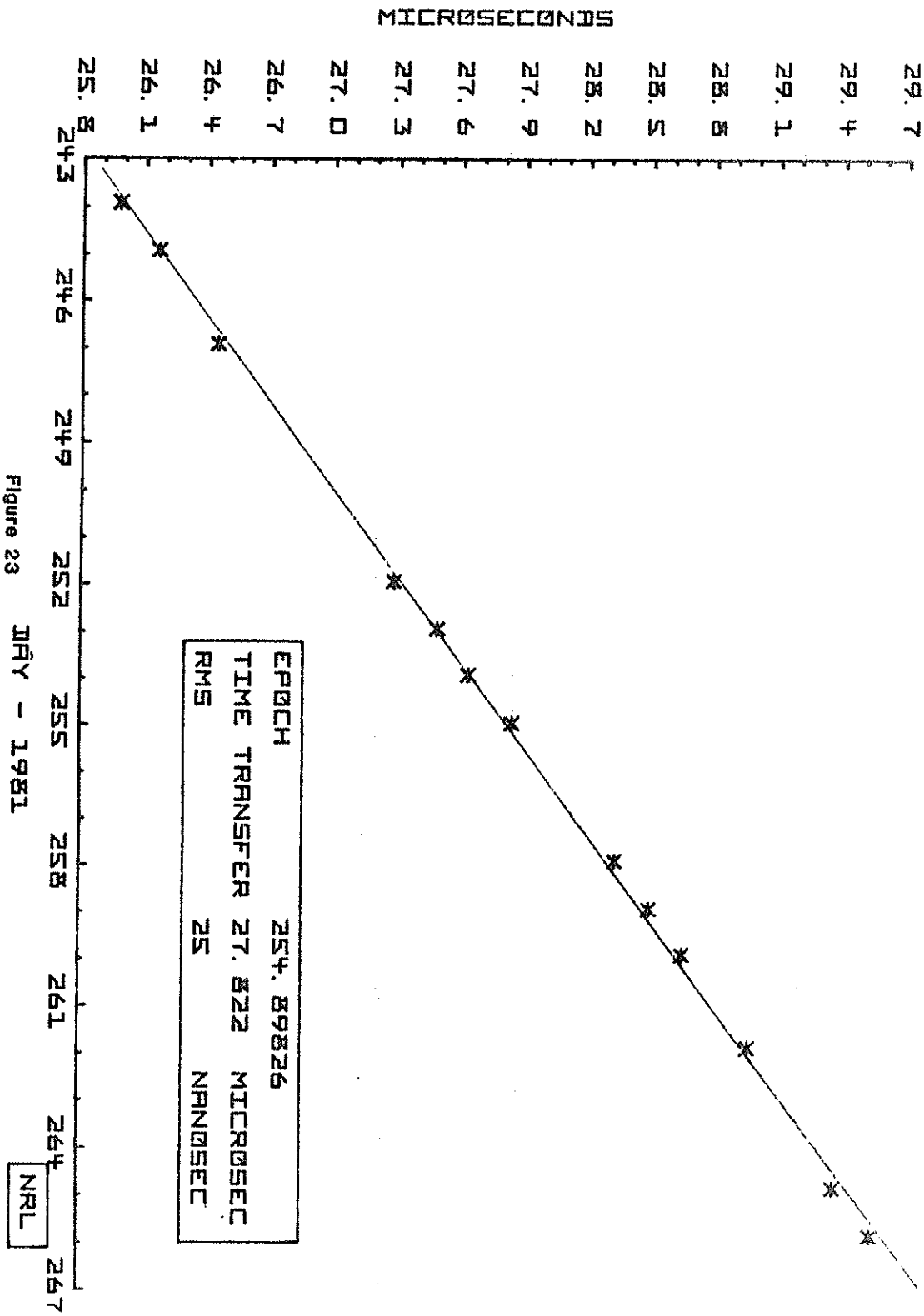

Figure 23 MAY - 1981

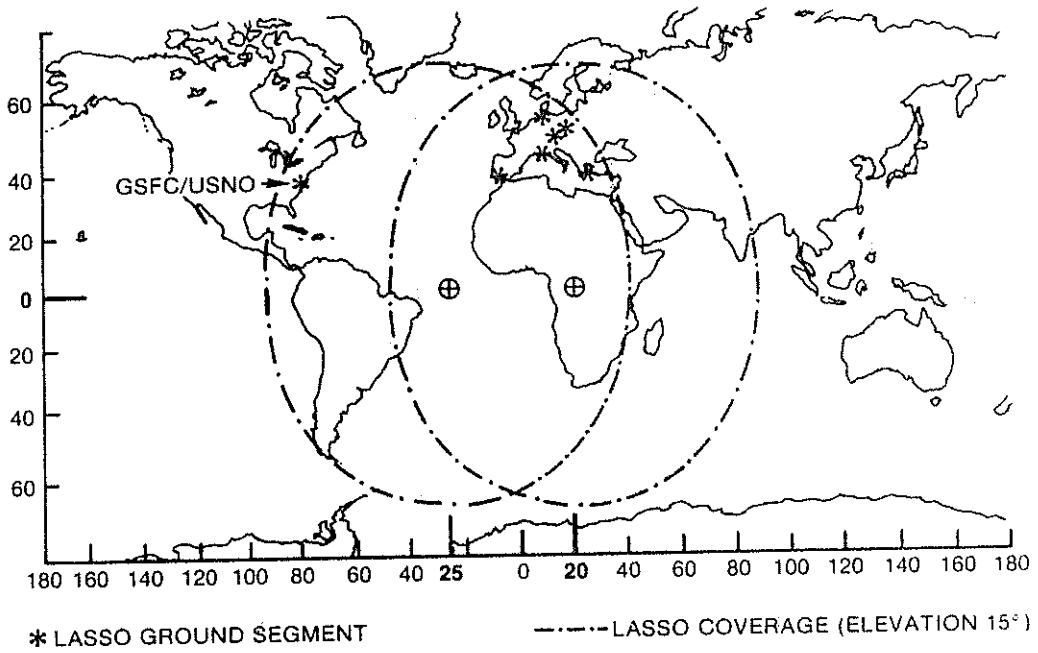

Figure 24. Provisional LASSO Coverage Zones

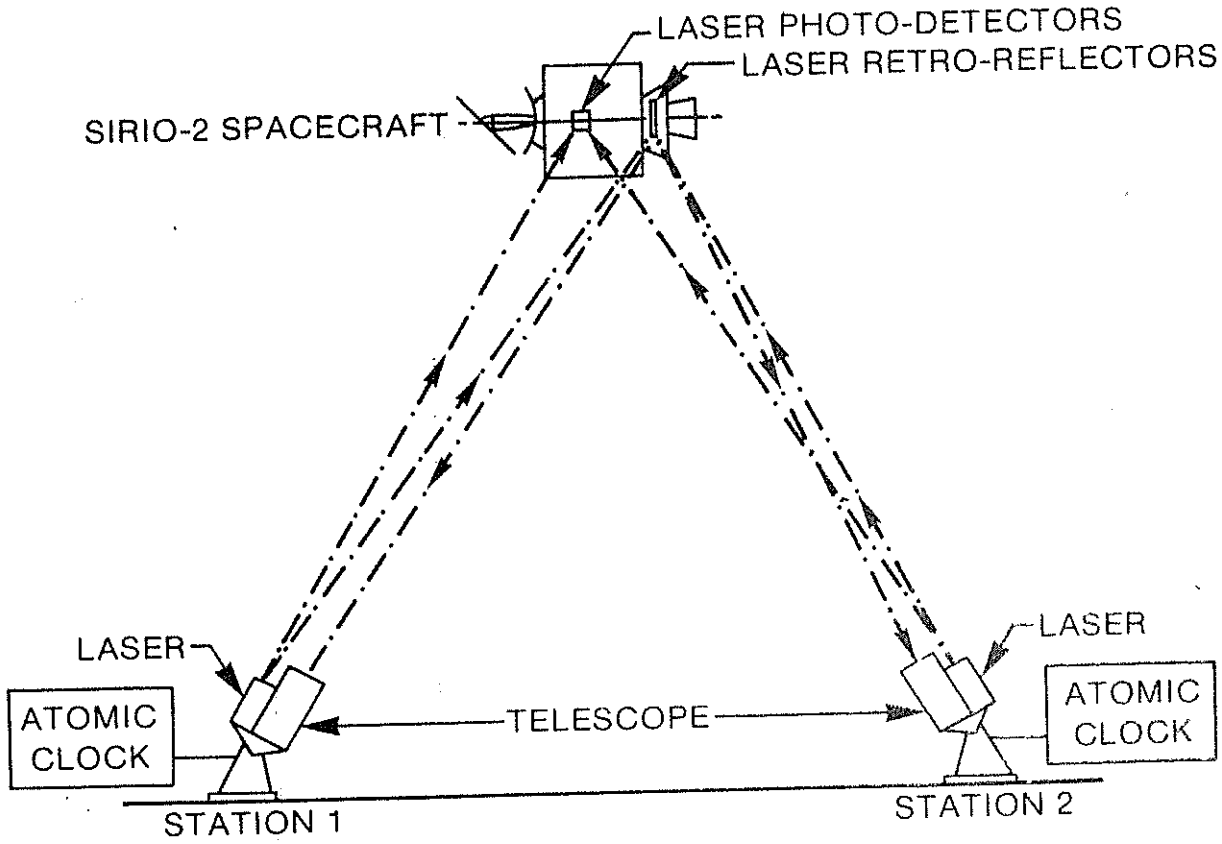

Figure 25. Schematic Diagram of LASSO Experiment

TRANSIT/NOVA SYSTEM WORLDWIDE TIME DISSEMINATION POTENTIAL CAPABILITY

LAUREN J. RUEGER
THE JOHNS HOPKINS UNIVERSITY APPLIED PHYSICS LABORATORY
JHU/APL
JOHNS HOPKINS ROAD
LAUREL, MD 20707

ABSTRACT

The Navy Navigation Satellite System (NNSS) has been in continuous operation providing UTC time marks at even two minutes since 1963. These time marks are presently traceable to the United States Naval Observatory (U.S.N.O.) master clock to uncertainties of 10 to 50 microseconds; a new spacecraft, (NOVA) was recently launched that has the potential capability of time mark traceability to less than 50 nanoseconds error to users anywhere in the world.

SYSTEM DESCRIPTION: Polar orbiting satellites at 600 nautical miles altitude transmit 150 and 400 MHz carriers modulated with a data message that mathematically describes the orbit position as a function of time. The data message is a prediction of the satellite position based on data from fixed ground stations making precise measurements of the frequency shift in the 150/400 MHz carriers as the spacecraft passes each ground station. There is sufficient information in the frequency shift on the received carriers to calculate the geometric position of the satellite relative to any receiving station. Therefore, knowing where the satellite is and knowing your position relative to the satellite provides a navigation fix. Part of this navigation solution provides the propagation path length at each two minute mark between the satellite and the ground-based receiver from which a time mark correction can be determined for setting local ground clocks.

OSCAR

The modulation in use since 1963 is recovered in a receiver phase-locked to the carrier as $\pm 60^{\circ}$ phase modulation in a binary code

bit (Fig. 1) period of 19.6 milliseconds (approximately 50 bits per second). The phase modulation is generated in T^2L logic with rise times of 20 nanoseconds. Antennas receiving signals from the overhead hemisphere provide signals at about — 120 dBm $^{+0}_{-20}$; the signal level fluctuations are due to multipath, and Faraday rotation, of the propagated signal and is due to variations in the signal polarization and attitude of the spacecraft. The time marks are kept in step with UTC by planned deletions of cycles in the clock divider circuits (Fig. 2); the steps being 9.6 μsec in size and occurring approximately 56 times each 2 minutes. Successive two minute periods will vary + or - one count from the average number of deletions. Therefore, to realize time from such a clock, it is desirable to average as many two minutes marks as possible. Seven or 8 time marks can be recovered each time the spacecraft passes the receiving station. Typically 2 successive revolutions are visible each 12 hours. Therefore, in 3 days as many as 84 time marks can be averaged.

$\frac{9.6}{\sqrt{42}}$ = 1.48 μs is the timing uncertainty W/O oscillator drift

2×10^{-11}/Day → 1.7 μs/DAY is a typical drift rate of orbiting oscillators and is predictable to

$\pm 2 \times 10^{-13}$ → 17 ns/DAY

2×10^{-12}/Day → 0.17 μs/DAY would be considered to be a low rate for an oscillator in orbit.

NOVA

The new generation of spacecraft for NNSS, has a much improved reference oscillator and a programmable synthesizer to normalize the frequency against drift so that a fixed divider chain drives the clock without any deletions of cycles. The same modulation for message data is used, however, another higher frequency modulation has been designed into the system 1.6 MHz bit rate for a pseudo random code (PRN) that repeats every 19.6 ms in synchronism with the message data. The NOVA timing chain is shown in (Fig. 3).

Experiments performed in 1977 using receivers modified to recover the PRN code on the 2 minute marks have demonstrated a 3 day average at each of two stations permitted time transfer at the 40 ns level. The experiment was set up at U.S.N.O. in Washington, D.C. and the National Bureau of Standards (NBS) in Boulder, Colorado. The reference measurements were two clock trips bracketing the experiment, one of which had probable errors of less than 3 ns, the other clock trip had errors as large as 25 ns.

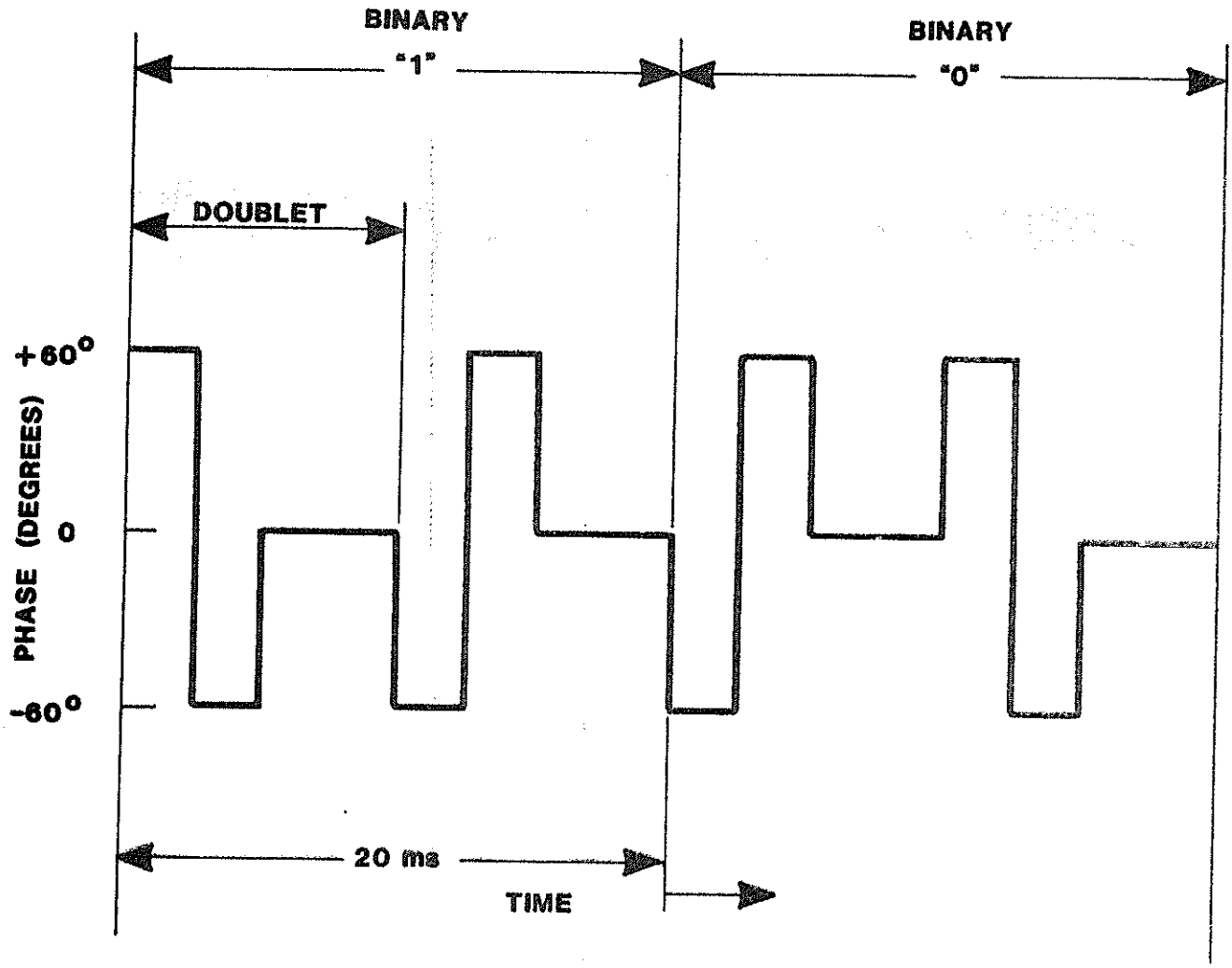

Fig. 1. MODULATION CHARACTERISTICS IN BINARY CODED FORM

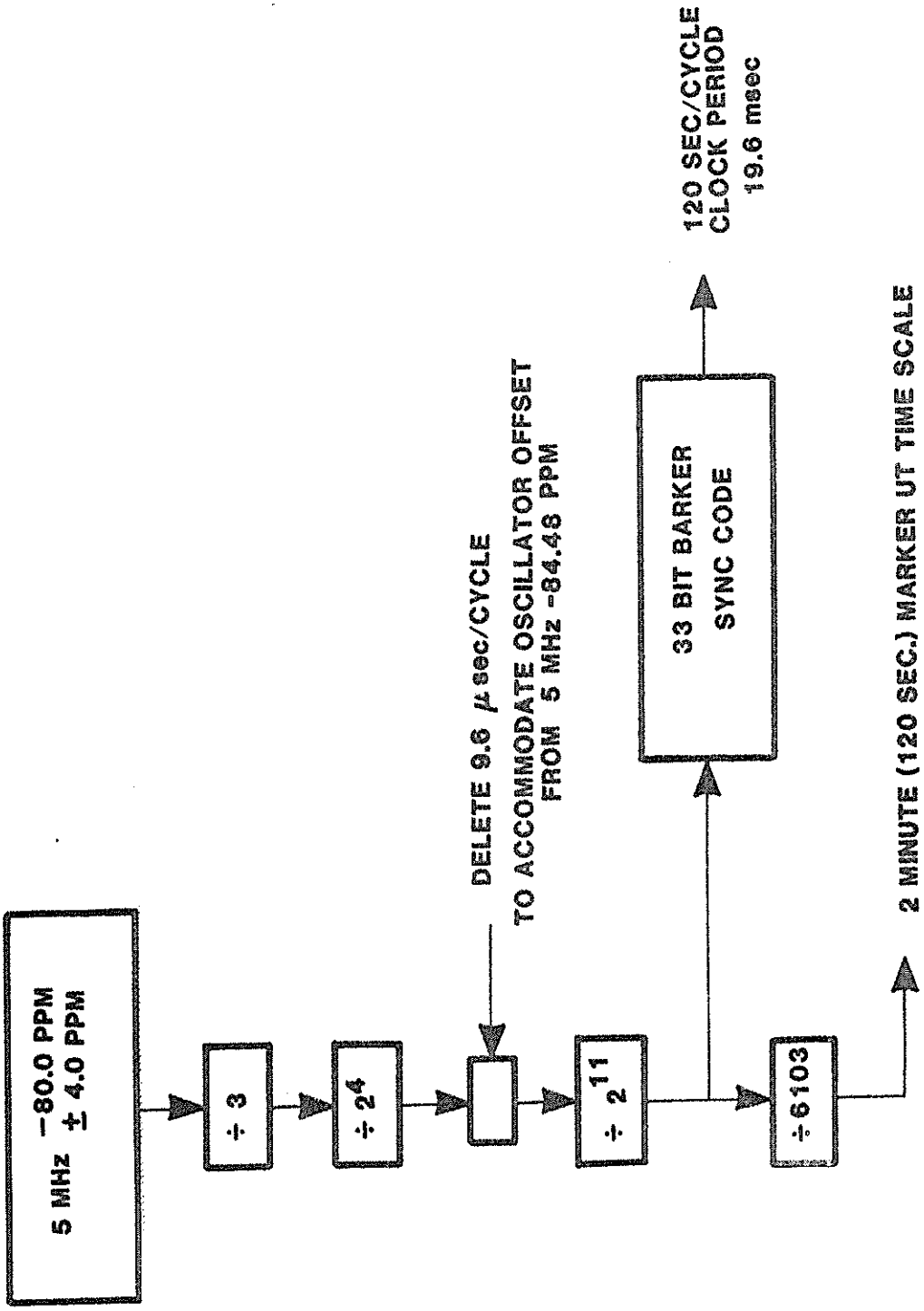

Fig. 2. OSCAR SPACECRAFT TIMING CHAIN

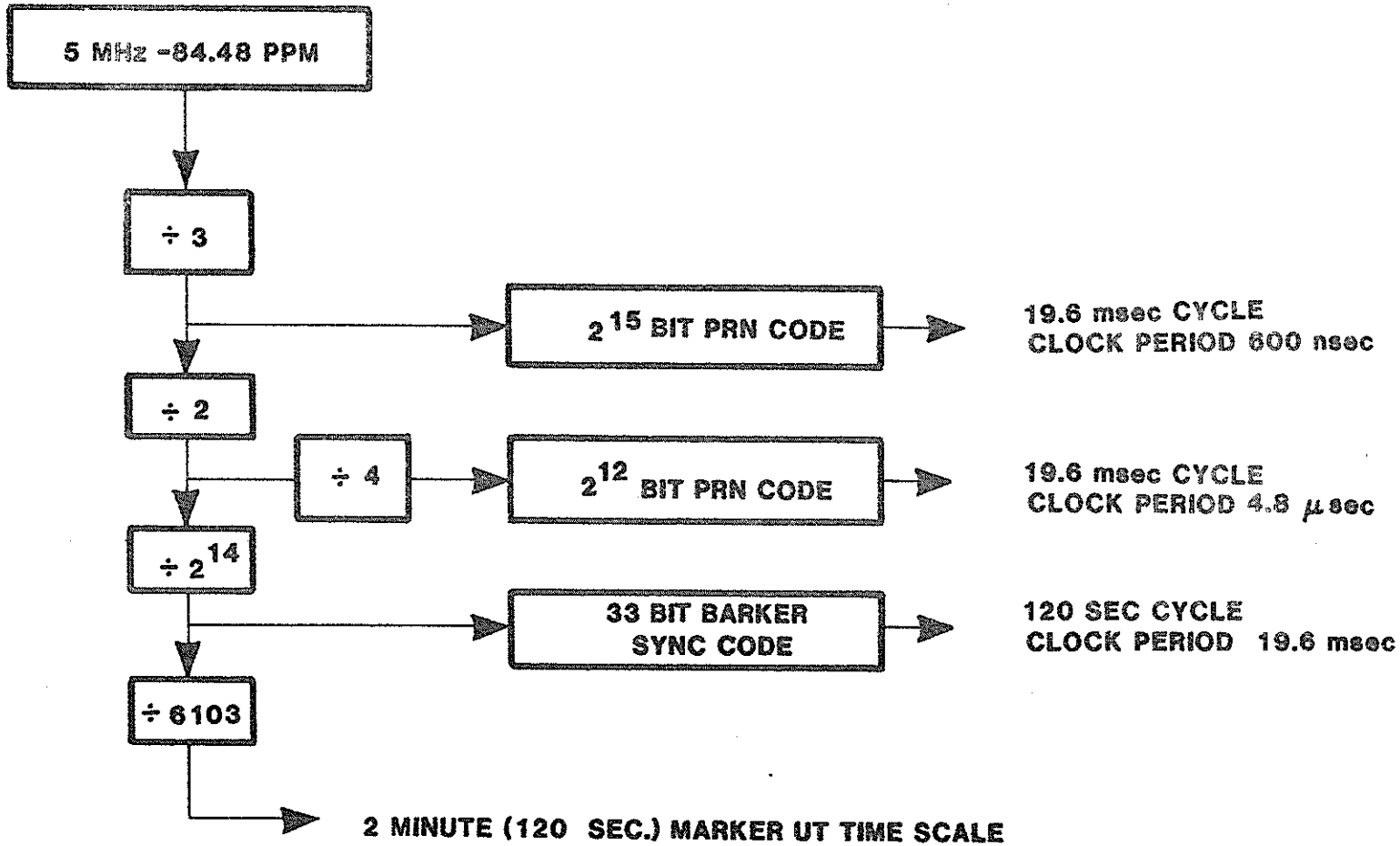

Fig. 3. NOVA SPACECRAFT TIMING CHAIN

Ground test data before launch on the satellite oscillators (Fig. 4) showed that in 3 days the clock could be steered to errors less than 50 ns and after 1 week the clock could be steered to within 2 ns of the reference clock using single measurements spaced 12 hours apart. The algorithm to steer the clock has Kalman filtering and clock modeling to accommodate the typical Allan variance of the specific oscillator being steered.

RECEIVERS

Since Pseudo Random Noise (PRN) modulation is not required to operate the NOVA satellite in the navigation mode, no plans to turn on PRN modulation exist. There is a commercial source for the standard OSCAR signal modulation time recovery priced between $10,000 and $20,000 depending on the optional features desired. Frequency & Time Systems, Inc. calls the receiver Model T-200. Units of these designs are operating at the U.S.N.O. and at several other sites in the U.S. The original Model T-200 receivers have Right Circular Polarized 400 MHz antenna and the antenna must be changed to either linear or Left Circular Polarized to recover NOVA signals.

NOVA PRN

The NOVA PRN modulation is expected to be turned on for a short period of operational tests in the near future as a diagnostic tool to make precision measurements on the oscillator performance in orbit. It is desired to determine the in-orbit predictability of drift rates as a reference mark for this oscillator and to examine the resolution to which the drift rates can be canceled and indexed to UTC time. The single measurement time resolution with PRN can be as small as 1 nanosecond with the laboratory instrumentation available at JHU/APL. Clock steerage is a software function; the operators of the spacecraft system need only know the clock corrections to be made and do not have to have direct access to the precision measurement receivers. Eventually, only one master clock facility like the U.S.N.O. would need to have the precision clock reception instruments to control the NNSS NOVA satellite.

If the remote site to be timed can see the exact same 2 minute time marks as the reference time station and measurements are made when the ionospheric activity is low (i.e. at night), the system can function at the 1 to 10ns level of time transfer.

If a valid requirement develops for the NNSS PRN timing system, it is understood that the U.S.N.O. would accept the monitoring role to obtain clock steerage data for the operational system. The use of the clock error data to steer the clock in NOVA satellites is within the current operating charter of Naval Astronautics Group (NAVASTROGRU) who control the NNSS.

TIP-III OSCILLATOR AND IPS LABORATORY TESTS

TIME STEERING:

- 50 nsec AFTER THREE DAYS
- 1-2 nsec AFTER SEVEN DAYS

Fig. 4. TIP-III TIME STEERING RESULTS